

# 1 **Understanding aerosol composition in a tropical inter-Andean valley** 2 **impacted by agro-industrial and urban emissions**

3

4 Lady Mateus-Fontecha<sup>1</sup>, Angela Vargas-Burbano<sup>1</sup>, Rodrigo Jimenez<sup>\*1</sup>, Nestor Y. Rojas<sup>1</sup>, German Rueda-  
5 Saa<sup>2</sup>, Dominik van Pinxteren<sup>3</sup>, Manuela van Pinxteren<sup>3</sup>, Khanneh Wadinga Fomba<sup>3</sup>, Hartmut Herrmann<sup>3</sup>

6

7 <sup>1</sup> Universidad Nacional de Colombia – Bogota, Department of Chemical and Environmental Engineering, Air Quality Research  
8 Group, Bogota, DC 111321, Colombia

9 <sup>2</sup> Universidad Nacional de Colombia – Palmira, Department of Engineering and Management, Environmental Prospective,  
10 Research Group, Palmira, Valle del Cauca 763533, Colombia

11 <sup>3</sup> Leibniz Institute for Tropospheric Research (TROPOS), Atmospheric Chemistry Department (ACD), Permoserstrasse. 15,  
12 04318, Leipzig, Germany.

13 *Correspondence to:* Rodrigo Jimenez ([rjimenezp@unal.edu.co](mailto:rjimenezp@unal.edu.co))

## 14 **Abstract.**

15 Agro-industrial areas are frequently affected by various sources of atmospheric pollutants that have a negative impact on public  
16 health and ecosystems. However, air quality in these areas is infrequently monitored because of their smaller population  
17 compared to large cities, especially in developing countries. The Cauca River Valley (CRV) is an agro-industrial region in  
18 Southwest Colombia, where a large fraction of the area is devoted to sugarcane and derivative production. The CRV is also  
19 affected by road traffic and industrial emissions. This study aims to elucidate the chemical composition of particulate matter  
20 fine mode (PM<sub>2.5</sub>) and to identify the main pollutant sources before source attribution. A sampling campaign was carried out  
21 at a representative site in the CRV region, where daily-averaged mass concentrations of PM<sub>2.5</sub> and the concentrations of water-  
22 soluble ions, trace metals, organic and elemental carbon, and various fractions of organic compounds (carbohydrates, n-  
23 alkanes, and polycyclic aromatic hydrocarbons – PAHs) were measured. The mean PM<sub>2.5</sub> was  $14.4 \pm 4.4 \mu\text{g m}^{-3}$ , and the most  
24 abundant constituent was organic material ( $52.7\% \pm 18.4\%$ ), followed by sulfate ( $12.7\% \pm 2.8\%$ ), and elemental carbon ( $7.1\%$   
25  $\pm 2.5\%$ ), which indicates secondary aerosol formation and incomplete combustion. Levoglucosan was present in all samples  
26 with a mean concentration of ( $113.8 \pm 147.2 \text{ ng m}^{-3}$ ) revealing biomass burning as a persistent source. Mass closure using the  
27 EC tracer method explained 88.4% of PM<sub>2.5</sub>, whereas the organic tracer method explained 70.9% of PM<sub>2.5</sub>. We attribute this  
28 difference to the lack of information of specific organic tracers for some sources, both primary and secondary. Organic material

29 and inorganic ions were the dominant groups of species (79% of PM<sub>2.5</sub>). OM<sub>prim</sub> and OM<sub>sec</sub> ~~from the EC-tracer method~~  
 30 contribute 24.2% and 28.5% to PM<sub>2.5</sub>. Inorganic ions as sulfate, nitrate and ammonia constitute 19.0%; EC<sub>s</sub> 7.1%; dust,  
 31 3.5%; PBW<sub>s</sub> 5.3%; and TEO<sub>s</sub> 0.9% of PM<sub>2.5</sub>. The aerosol was acidic, with a pH of 2.5 ± 0.4, mainly because of the abundance  
 32 of organic and sulfur compounds. Diagnostic ratios and tracer concentrations indicate that most PM<sub>2.5</sub> was emitted locally and  
 33 had contributions of both pyrogenic and petrogenic sources, that biomass burning was ubiquitous during the sampling period  
 34 and was the main source of PAHs, and that the relatively low PM<sub>2.5</sub> concentrations and mutagenic potentials are consistent  
 35 with low-intensity, year-long BB and sugarcane PHB in CRV.

36

37

38 Keywords: agro-industry; pre-harvest burning; PM<sub>2.5</sub>; chemical speciation; ~~principal component analysis~~; Northern South  
 39 America

40

#### 41 1. Introduction

42 Urban and suburban locations, with moderate to high population densities, are exposed to air pollutant emissions, including of  
 43 fine particulate matter (PM)<sub>2.5</sub> from industry, road traffic, and other anthropogenic activities. Suburban areas may also be  
 44 impacted by emissions from agricultural activities (Begam et al., 2016). Air quality in areas under these conditions is  
 45 infrequently monitored, particularly in developing countries, despite the extensive use of highly emitting practices, including  
 46 intensive use of insecticides and pesticides, fire for land and crop management, and diesel-based mechanization (Aneja et al.,  
 47 2008, 2009). Agricultural sources emit pollutants, such as volatile organic compounds (VOC), which are precursors of  
 48 tropospheric ozone (Majra, 2011) and secondary organic aerosols (SOA) (Majra, 2011). Most agricultural activities also emit  
 49 PM<sub>2.5</sub> (solid and liquid particles with aerodynamic diameters smaller than 2.5 μm), which may contain black carbon (BC)  
 50 and toxic and carcinogenic pollutants, e.g., polycyclic aromatic hydrocarbons (PAHs). Other agricultural activities, including  
 51 mechanized land preparation, sowing and harvesting, consume significant volumes of fossil fuels, particularly diesel, and emit  
 52 trace gases (including CO<sub>2</sub>, CO, SO<sub>2</sub>, NO<sub>x</sub>, NH<sub>3</sub>, VOC) that also generate O<sub>3</sub> and SOA, all of which affect human health and  
 53 climate (Yadav and Devi, 2019). Furthermore, agricultural operations are a significant source of nitrogen-containing trace  
 54 gases (NO<sub>2</sub>, NO, NH<sub>3</sub>, N<sub>2</sub>O) that are released from fertilizers, livestock waste, and farm machinery into the atmosphere (Sutton  
 55 et al., 2011). Also, poultry and pig farming are high emitters of sulfur compounds, particularly H<sub>2</sub>S.

56

57 The Cauca River Valley (CRV) is an inter-Andean valley in Southwest Colombia with a flat area of 5287 km<sup>2</sup> (248-km long  
 58 by 22-km mean width), a mean altitude of 985 m MSL (Figure 1). CRV is bounded by the Colombian Andes Western and  
 59 Central Cordilleras, and is located at ~120 km from the Pacific Ocean. CRV encompasses the cities of Cali, Colombia's third-  
 60 largest city with 2.2 million inhabitants (inhab), Yumbo (129 thousand inhab), an important industrial hub, and Palmira (313

Con formato: Resaltar

Con formato: Resaltar

61 [thousand inhabitants](#)), an important agro-industry center. [Industry is also present in the other major CRV cities \(Tuluá, Cartago,](#)  
62 [Jamundí, and Buga\).](#)

63

64 CRV hosts a highly efficient, resource-intensive sugarcane agro-industry with one of the highest biomass yields (up to 120 ton  
65 ha<sup>-1</sup>) and the highest sugar productivities in the world (~13 ton sugar ha<sup>-1</sup>) (Asocaña, 2018, 2019). Sugarcane [farming](#),  
66 [harvesting](#), and transport to mills are all mechanized and use diesel as fuel. Besides, all the sugarcane bagasse is used, either  
67 [to produce heat and electric power \(cogeneration\) or as feedstock to the local paper industry. Moreover, although pre-harvest](#)  
68 [burning is being phased out in CRV, one-third of the sugarcane area in 2018 was burned prior to harvesting. Other significant](#)  
69 [agro-industrial activities in CRV include poultry and livestock production.](#) CRV is [also](#) the third largest [poultry](#) producer [of](#)  
70 [poultry](#) (351,104 ton yr<sup>-1</sup>), and the first egg producer (4,559 million units per year) in Colombia (Min.Agricultura, 2020). In  
71 addition, CRV produces 15.1% of Colombia's pork meat (over 1 million pigs in stock) (Min.Agricultura, 2019) and 1.8% of  
72 national beef production (467,782 heads in stock) (Min.Agricultura, 2018). [Poultry and livestock production are significant](#)  
73 [sources of H<sub>2</sub>S and NH<sub>3</sub>. Besides a long-time established energy-intensive industry, there are also a variety of smaller](#)  
74 [industries, including Other no-registered sources are a brick kilns and coal kiln agricultural waste burning.](#) Regarding mobile  
75 sources, there are nearly 2 million vehicles (1,951,638 vehicles) registered in CRV ([RUNT, 2021](#)). These include the standard  
76 urban categories along with off-road unregulated farming machinery. The sugarcane agroindustry uses multi-car trailers towed  
77 by diesel-powered tractors, with enough annual activity to be considered an independent source (the activity of which is  
78 proportional to the sugarcane harvested area and the distance to sugar mills). Overall, CRV mobile sources consumed 772  
79 million L of gasoline and 590 million L of diesel in 2018 (SICOM, 2018). Moreover, the local airport, [the most important in](#)  
80 [southwest Colombia, located](#) very close to Palmira, [is of the Colombian west hub, which](#) handled 1.3 million passengers in  
81 2019 (Aerocivil, 2019). [Also, small aircraft is used for pesticide application, with 147 applications over sugarcane fields and](#)  
82 [27 applications over corn fields, for a total of 1657 ha of sugarcane and corn were fumigated in 2020 using small aircraft](#)  
83 (Aerocivil, 2020). [The other main economic line in CRV is the manufacturing industry, located mainly in the seven largest](#)  
84 [CRV cities: Cali, Tuluá, Cartago, Jamundí, Yumbo, Buga and Palmira.](#)

85

86 For this research, we [made prepared](#) a preliminary [estimation of the](#) aggregated PM<sub>10</sub> emission [inventories in for](#) CRV by  
87 putting together disparate source data, including from the stationary source emission inventories of CRV's six largest cities  
88 (Cali, Tuluá, Cartago, Jamundí, Palmira, Yumbo and Buga), Cali's and other cities', mobile source emission inventories,  
89 and [an estimation our an estimation](#) of sugarcane pre-harvest burning (PHB) [and other point, linear and area sources](#) (Table  
90 [S14](#)). [According to Our preliminary inventory estimates, indicates that](#) the manufacturing industry is [by far](#) the main PM<sub>10</sub>  
91 emitter in CRV, with annual emissions of [~8.244 kt<sub>PM10</sub>a<sup>-1</sup>](#). PM<sub>10</sub> emissions from mobile sources ([~1.434 kt<sub>PM10</sub>a<sup>-1</sup>](#)  
92 year<sup>-1</sup>) and open-field sugarcane pre-harvest burning ([1.7 kt<sub>PM10</sub>a<sup>-1</sup>](#)) are a factor [~53 and ~7](#) smaller [than](#)  
93 [manufacturing industry, respectively. The emissions of inorganic and organic secondary aerosol precursors are also significant.](#)

Con formato: Subíndice

Con formato: Subíndice

Con formato: Subíndice

Con formato: Subíndice

94 We estimate that 30.1 Gg of SO<sub>2</sub> are annually emitted in CRV (41% from sugar mills and other agro-industries, 32% from  
 95 food industries, and 9% from cement, ceramic and asphalt production). Emissions of volatile organic compounds (VOCs) are  
 96 very similar (34.7 Gg yr<sup>-1</sup>). Although a significant number of coal-fired boilers have been converted to natural gas, CRV's  
 97 sulfur-rich coal (1.4-4% total S) is still an important industrial fuel. It must be stressed that this is a preliminary, not fully  
 98 updated, regional inventory. Nonetheless, it is worth mentioning the following: 1) The available information was insufficient  
 99 for disaggregating the fine-mode PM emissions estimating total (PM<sub>2.5</sub>) emissions; 2) No emission data were inventory was  
 100 available on Palmira, the city where our measurement site is located; 3) The stationary emission inventory of Yumbo, an  
 101 industrial hub with the largest industrial activity, is not fully developed and, therefore, outdated and very likely  
 102 suboverestimated, particularly as a significant fraction of coal-fired boilers there have been converted to natural gas. The  
 103 multiplicity, disparity, and uncertainty of sources are indicative of the complexity of the PM<sub>2.5</sub> source identification,  
 104 quantification, and location tasks.

Con formato: Superíndice

106 The determination of the particulate matter (PM) chemical composition is instrumental for the apportionment of pollutant  
 107 sources. Most field measurement-based studies have been conducted in North America, Europe, and Asia (Karagulian et al.,  
 108 2015). The number of studies in Latin America and the Caribbean (LAC) is much smaller and have focused on the chemical  
 109 composition of PM<sub>10</sub> (Pereira et al., 2019; Vasconcellos et al., 2011), as well as the PM source apportionment in urban areas  
 110 of Colombia (Ramírez et al., 2018; Vargas et al., 2012), Chile (Jorquera and Barraza, 2012, 2013; Villalobos et al., 2015),  
 111 Costa Rica (Murillo et al., 2013) and Brazil (de Andrade et al., 2010). The number of studies that involve agro-industrial  
 112 sources and their impact on suburban areas is smaller. These include the Indo-Gangetic plain (Alvi et al., 2020), the Sao Paulo  
 113 State in Brazil (Gonçalves et al., 2016; Urban et al., 2016), Ouagadougou in Burkina Faso (Boman et al., 2009), the Anhui  
 114 Province in China (Li et al., 2014), for which the chemical composition of PM<sub>2.5</sub> and some of its sources have been identified.  
 115 Likewise, regions in South America with sugarcane agroindustry, such as Mexico (Mugica-Alvarez et al., 2015; Mugica-  
 116 Álvarez et al., 2016, 2018) and Brazil (de Andrade et al., 2010; De Assuncao et al., 2014; Lara et al., 2005; Pereira et al., 2017)  
 117 have also reported on their agro-industry impact on PM<sub>2.5</sub> levels at nearby population centers. They are very few studies on  
 118 agricultural air quality pollution in agro-industrial areas in of Colombia. Most notably, Romero et al., (2013) measured PAHs  
 119 and metals in PM<sub>10</sub>. Most of the studies above identified biomass burning and fossil fuel combustion as significant PM sources,  
 120 and some also identified industrial and fertilizer as relevant.

Con formato: Subíndice

Código de campo cambiado

Código de campo cambiado

Código de campo cambiado

Código de campo cambiado

Código de campo cambiado

122 This research aimed to characterize the chemical composition of PM<sub>2.5</sub> at a representative location in the CRV, including EC,  
 123 primary and secondary OC, ions, trace metals, and specific molecular markers, such as PAH/PAHS, n-alkanes, and  
 124 carbohydrates, as well as the relationships among these components and with emission sources. Diagnostic ratios were used  
 125 to identify the most important PM<sub>2.5</sub> components and as a tool for preliminary pollutant source attribution, including primary  
 126 and secondary aerosols generated by or associated with sugarcane pre-harvest burning PHB. We believe that in the CRV case,

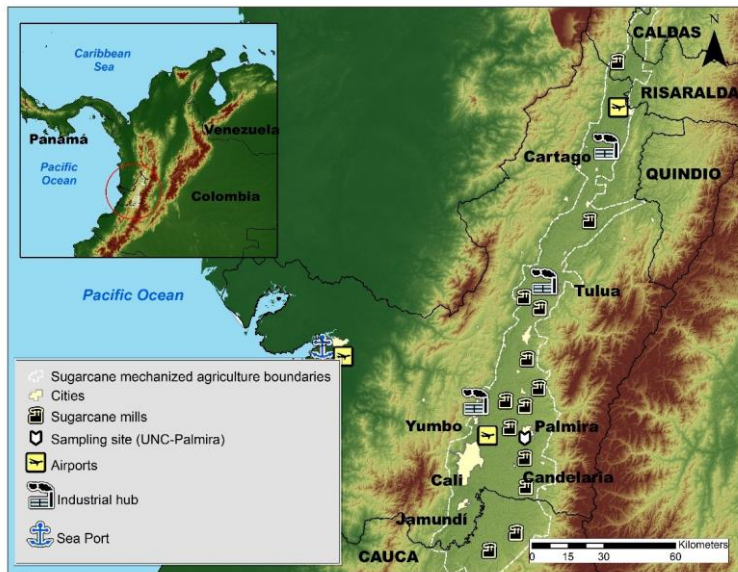
127 this analysis is needed prior to source apportionment with receptor models for three reasons: 1) This is the first comprehensive  
128 investigation of PM composition in the CRV (prior studies included two types of components at most); 2) There are no suitable  
129 chemical profiles for some pollutant sources, particularly sugarcane PHB; 3) Our measurements dataset is just barely large  
130 enough for profile-free receptor modeling (positive matrix factorization). [We expect that this study also motivates future](#)  
131 [research on source apportionment in the region.](#) Our results are particularly relevant for urban communities and atmospheres  
132 impacted by large-scale intensive agriculture and industrial emissions, particularly in developing countries, especially in Latin  
133 America where PM composition information is still scarce (Liang et al., 2016).

134

## 135 2. Methods

### 136 2.1. Description of the sampling site

137 The sampling site was located on the rooftop of an 8-story administrative building at the Palmira Campus of Universidad  
138 Nacional de Colombia (3°30'44.26" N; 76°18'27.40" W, 1065 m altitude), about 27 m above the ground. The campus is located  
139 on the western outskirts of Palmira's urban area and is surrounded by short buildings on the east, and extensive sugarcane  
140 plantations, several sugar mills, and other industries elsewhere. Palmira is located at ~27 km northeast of Cali and ~22 km  
141 southeast of Yumbo, an important industrial hub. The Pacific Ocean coastline stretches at ~120 km across the Western  
142 Cordillera, as shown in [Figure 1](#)~~Figure 1~~, where operates one of the busiest international trade seaports in Colombia ~~the country~~  
143 (López, 2017). Most of the freight is transported by diesel-powered trucks. Road traffic is also substantial within the CRV,  
144 with Bogota and along the Pan-American highway that connects Colombia with other South American countries (Orozco et  
145 al., 2012).



146

147 Figure 1. Map of the Cauca River Valley (CRV). The inset shows the location of CRV in Colombia and in Northern South  
 148 America. The map shows the main cities in CRV, including Palmira (312 thousand inhabitants), our measurement site, Cali,  
 149 the largest city in the southwest of Colombia, Yumbo, an industrial hub, and the main highways. Sugar mills, which produce  
 150 sugar, bio-ethanol, and electric power are also shown. The dashed-line defined area is CRV's flattest (slope < 5%) bottomland,  
 151 where mechanized, intensive sugarcane agriculture takes place. Significant diesel combustion emissions occur along the  
 152 Buenaventura highway because it is one of the busiest ports in Colombia.

153

154 The Andes Cordillera splits into three south-to-north diverging mountain ranges (Western, Central, and Eastern Cordilleras)  
 155 near the Colombia-Ecuador border (see Figure 1). The Western Cordillera separates the CRV from the Colombian Pacific  
 156 Ocean watershed, the rainiest region on Earth (Hernández and Mesa, 2020). The elevated precipitation in this basin (Mesa and  
 157 Rojo, 2020) is due to the presence of a Walker cell convergence zone at the surface, persistent under neutral and La Niña  
 158 conditions. This synoptic feature is one of the most important determinants of atmospheric circulation in Colombia, with  
 159 prevailing east-to-west winds in the lower troposphere along with upper troposphere return winds (Mesa and Rojo, 2020). The  
 160 Andean Cordilleras are nevertheless effective barriers to the Walker circulation near the CRV surface (Lopez and Howell,  
 161 1967; Mesa S. and Rojo H., 2020). The elevated humidity in the Pacific Ocean watershed and the closeness of the two Andes

162 branches drive a zonal regional circulation pattern, consisting ~~in~~ of west-to-east anabatic winds over the Pacific slope of the  
163 Western Cordillera during the daytime followed by rapid katabatic winds in the late afternoon (Lopez and Howell, 1967).  
164 These winds rapidly ventilate the CRV during the late afternoon – early evening period on an almost regular basis. CRV is  
165 wide (~22 km) and long (~248 km) enough to develop a valley-mountain wind circulation pattern during the daytime. Winds  
166 are very mild during this time period and expected to be highly dispersive, i.e. with high turbulence intensities (Ortiz et al.,  
167 2019). The arrival of the katabatic “tide” in the late afternoon wipes the valley-mountain wind pattern out (Lopez and Howell,  
168 1967).

## 169 2.2. Sampling protocols

170 The sampling campaign was conducted between July 25<sup>th</sup> and September 19<sup>th</sup>, 2018. PM<sub>2.5</sub> aerosol particles (aerodynamic  
171 diameter < 2.5 µm) were collected on Teflon and quartz fiber filters simultaneously for 23 h (from 12:00 local time – LT – to  
172 the next day at 11:00 LT), using 2 in-tandem low-volume samplers (ChemComb speciation samplers, R&P). Each sampler  
173 used an independent pump set at a flow rate of 14 L min<sup>-1</sup>. For both types of filters, three lab blank filters without exposure  
174 were analyzed. Quartz filters were pre-baked at 600 °C for 8 h before sampling to eliminate contaminant trace hydrocarbons.  
175 In total, 45 samples were collected. Prior to and after exposure, the filters were conditioned at constant humidity (36±1.5%  
176 relative humidity) and temperature (24 ± 1.2 °C) for 24 h before being weighing on a microbalance (Sartorius, Mettler Toledo)  
177 with a 199.99 g capacity and 10 µg resolution. PM<sub>2.5</sub>-loaded filters were saved at Petri boxes previously prepared to avoid  
178 cross-contamination of organic species. The filters were subsequently stored at –20°C until analysis to reduce the volatilization  
179 of species such as ammonium nitrate and semi-volatile organic compounds. Blank quartz filters were pre-baked and stored  
180 following an identical procedure to exposed filters to collect samples. Blank Teflon filters were treated under the same  
181 conditions of storage, transport, and analysis as PM<sub>2.5</sub>-loaded filters.

182 Several frequent challenges can affect compound measurements in particle matter, including: 1) The absorption of some gases  
183 in the inlet's galvanic steel, which alters the gas and particle balance of the HNO<sub>3</sub> = NO<sub>3</sub>- system of particles collected. During  
184 the collecting of the samples for this study, no denuders were utilized. 2) Significant temperature changes during sampling and  
185 then in the conditioning before to filter weighing can cause ammonium nitrate to volatilize. Because the samples were collected  
186 at temperatures ranging from 17 to 33 C and then conditioned to 25 C, the equilibrium of the HNO<sub>3</sub> = NO<sub>3</sub>- system could be  
187 a source of ambiguity in the data reported here. The vaporization of some semi-volatile organic species throughout the sampling  
188 and storage period, as well as the absorption of organic gases over the filter material, are two additional sources of uncertainty.

189  
190

191 By differential weighing, mass concentrations were determined from the Teflon filters. It's worth mentioning that during the  
192 sampling period, 1888 sugarcane PHB episodes occurred. This register was made by the regional environmental agency (CVC,  
193 as per its acronym in Spanish), using information from sugar mills about PHB events. The vast majority of these events were  
194 intentional, controlled, size-limited (~6 ha median area), and brief (~25-minute median duration) (Fig S1).

Con formato: Fuente: (Predeterminada) Times New Roman,  
10 pto, Color de fuente: Automático

195 **2.3. Analytical methods**

196 The quartz-fiber filter samples were analyzed for ions, metals, elemental and organic carbon, and speciation of the  
197 carbonaceous fraction. The Teflon-membrane filter samples were analyzed for metals.

198

199 Two circular pieces with an 8 mm diameter (100.5 mm<sup>2</sup>) were punched from each quartz and Teflon filter, following the  
200 method described by Wadinga Fomba et al., (2020), and extracted using 1 mL of ultrapure water (18 MΩ) in a shaker at 400  
201 rpm for 120 min. The extracts were filtered through 0.45 μm syringe filters (Acrodisc Pall). An aliquot of the solution was  
202 analyzed for inorganic (K<sup>+</sup>, Na<sup>+</sup>, NH<sub>4</sub><sup>+</sup>, Mg<sup>2+</sup>, Ca<sup>2+</sup>, Cl<sup>-</sup>, NO<sub>3</sub><sup>-</sup>, SO<sub>4</sub><sup>2-</sup>, NO<sub>2</sub><sup>-</sup>, PO<sub>4</sub><sup>3-</sup>, Br<sup>-</sup>, F<sup>-</sup>) and some organic ions (C<sub>2</sub>O<sub>4</sub><sup>2-</sup>,  
203 CH<sub>3</sub>O<sub>3</sub>S<sup>-</sup>, and CHO<sub>2</sub><sup>-</sup>) by ion chromatography (IC690 Metrohm; ICS3000, Dionex). Another aliquot was analyzed for  
204 carbohydrates, including levoglucosan, mannosan, and galactosan, as described by Inuma et al. (2009a). Organic and  
205 elemental carbon were determined from 90.0 mm<sup>2</sup> filter pieces following the EUSAAR 2 protocol (Cavalli et al., 2010), with  
206 a thermal-optical method using a Sunset Laboratory dual carbonaceous analyzer.

207

208 Seventeen metals, including K, Ca, Ti, V, Cr, Mn, Fe, Ni, Cu, As, Se, Sr, Ba, Pb, Sn, Sb, and Cu, were analyzed from Teflon  
209 (22 samples) and quartz (23 samples) filters by total reflection X-Ray Fluorescence Spectroscopy – TXRF (TXRF, PICOFOX  
210 S2, Bruker). Si was not determined as this element is part of the quartz filter substrate. Metals were analyzed from three 8-mm  
211 circular pieces punched from Teflon filters, which were digested a nitric and chloride acid solution for 180 min at 180 °C.  
212 After this, 20-μl aliquots of the digested solution were placed on the surface of polished TXRF quartz substrates along with  
213 10 μl of Ga solution, which served as an internal standard. This solution was left to evaporate at 100°C. The samples were  
214 measured at two angles with a difference of 90° between them to ensure complete excitation of metals. More details on the  
215 analytical technique can be found in Fomba et al. (2013).

216

217 Alkanes and PAHs were determined from two circular filter punches (6 mm diameter, 56.5 mm<sup>2</sup>), using a Curie-point pyrolyzer  
218 (JPS-350, JAI) coupled to a GC-MS system (6890 N GC, 5973inert MSD, Agilent Technologies). The chemical identification  
219 and quantification of the C<sub>20</sub> to C<sub>34</sub> n-alkanes, as well as the following organic species were performed using the following  
220 external standards (Campro, Germany): pristane, phytane, fluorene (FLE), phenanthrene (PHEN), anthracene (ANT),  
221 fluoranthene (FLT), pyrene (PYR), retene (RET), benzo(b)naphtho(1,2-d)thiophene (BNT(2,1)), cyclopenta(c,d)pyrene  
222 (CPY), benz(a)anthracene (BaA), chrysene(+Triphenylene) (CHRY), 2,2-binaphthyl (BNT(2,2)), benzo(b)fluoranthene (BbF),  
223 benzo(k)fluoranthene (BkF), benzo(e)pyrene (BeP), benzo(a)pyrene (BaP), indeno (1,2,3-c,d)pyrene (IcdP),  
224 dibenz(a,h)anthracene (DahA), and benzo(g,h,i)perylene (BghiP), coronene (COR), 9H-Fluorenone (FLO(9H)), 9,10-  
225 Anthracenedione (ANT (9,10)) and 1,2-Benzanthraquinone (BAQ (1,2)). Four deuterated PAHs, (acenaphthene-d10,  
226 phenanthrene-d10, chrysene-d12, and perylene-d12), and two deuterated alkanes (tetracosane-d50 and tetratriacontane-d70)



227 were used as internal standards, following the analytical method described by (Neusüss et al., 2000). For each analyzed  
 228 compound, the sample concentration was calculated by subtracting the average concentration of three blank filters from the  
 229 measured concentration.

#### 230 2.4. Diagnostic ratios and mass closure

231 The main PM<sub>2.5</sub> components were estimated from the concentrations of EC, OC, water-soluble ions (NO<sub>3</sub><sup>-</sup>, SO<sub>4</sub><sup>2-</sup>, NH<sub>4</sub><sup>+</sup>, and  
 232 Na<sup>+</sup>), and tracer metal concentrations (Ca, Ti, Fe, Ni, Cu, Zn, As, Se, Sb, Ba, and Pb) as follows: organic material (OM), EC,  
 233 ammonium sulfate ((NH<sub>4</sub>)<sub>2</sub>SO<sub>4</sub>), ammonium nitrate (NH<sub>4</sub>NO<sub>3</sub>), crustal material (dust), other trace elements oxides (TEOs),  
 234 and particle-bounded water (PBW). PM<sub>2.5</sub> closure is described by Eq 1 (Dabek-Zlotorzynska et al., 2011). We used the  
 235 Interagency Monitoring of Protected Visual Environment (IMPROVE) equations (Chow et al., 2015) to quantify the  
 236 concentrations of main compounds (Table 1). The aerosol particle bounded water content was estimated from the measured  
 237 ionic composition, relative humidity, and temperature, following the aerosol inorganic model (AIM) described by (Clegg et  
 238 al., 1998), which is available for running online at <http://www.aim.env.uea.ac.uk/aim/model2/model2a.php>. The  
 239 thermodynamic equilibrium of the system H<sup>+</sup>- NH<sub>4</sub><sup>+</sup> - Na<sup>+</sup> - SO<sub>4</sub><sup>2-</sup> - NO<sub>3</sub><sup>-</sup> - Cl<sup>-</sup> - H<sub>2</sub>O is described by AIM.

240

$$241 \text{ PM}_{2.5}(\text{mass closure estimated}) = \text{OM}_{\text{pri}} + \text{OM}_{\text{sec}} + \text{EC} + \text{NH}_4\text{SO}_4 + \text{NH}_4\text{NO}_3 + \text{Dust} + \text{TEO} + \text{SS} + \text{PBW} \quad \text{Eq (1)}$$

242 Table 1. Equations used to estimate the main components of PM<sub>2.5</sub>

Component	Equation	Reference
OM <sub>prim</sub>	$= f_1 \text{ OC}_{\text{prim}}$	(Chow et al., 2015) (Turpin and Lim, 2010)
OM <sub>sec</sub>	$= f_2 \text{ OC}_{\text{sec}}$	(El-Zanan et al., 2005)
SO <sub>4</sub>	$= \text{SO}_4^{2-}$	(Chow et al., 2015)
NO <sub>3</sub>	$= \text{NO}_3^-$	(Chow et al., 2015)
Dust	$= 1.63\text{Ca} + 1.94\text{Ti} + 2.42\text{Fe}$ (Assuming CaO, Fe <sub>2</sub> O <sub>3</sub> , FeO (in equal amounts) and TiO <sub>2</sub> )	(Chow et al., 2015)
PBW	$= k (\text{SO}_4^{2-} + \text{NH}_4^+)$	(Clegg et al., 1998)
TEO	$= 1.47[\text{V}] + 1.27[\text{Ni}] + 1.25[\text{Cu}] + 1.24[\text{Zn}] + 1.32[\text{As}] +$ $1.2[\text{Se}] + 1.07[\text{Ag}] + 1.14[\text{Cd}] + 1.2[\text{Sb}] + 1.12[\text{Ba}] +$ $1.23[\text{Ce}] + 1.08[\text{Pb}]$	(Snider et al., 2016)

243  $f_1 = 1.6$ . This factor was estimated considering the predominant sources.

244  $f_2 = 2.1$ . This factor was estimated by subtracting the non-carbon component of PM<sub>2.5</sub> from the measured mass.

245  $k = 0.32$  was calculated using the Aerosol Inorganic Model.

246

Con formato: Superíndice

Con formato: Superíndice

247 The EC tracer method was applied to estimate primary ( $OC_{prim}$ ) and secondary ( $OC_{sec}$ ) organic carbon (Lee et al., 2010). This  
 248 method utilizes EC as a tracer for primary OC, which implies that  $OC_{prim}$  from non-combustion sources is deemed negligible.  
 249 Primary and secondary OC can be estimated by defining a suitable primary OC to EC ratio ( $[OC/EC]_{prim}$ ). See Eq (2) and Eq  
 250 (3). We estimated the  $[OC/EC]_{prim}$  ratio as the slope of a Deming linear fit between EC and OC measurements. The term  $b$   
 251 corresponds to the linear fit intercept, which can be interpreted as the emitted  $OC_{prim}$  that is not associated with EC emissions.  
 252 This method is limited by the following assumptions: 1)  $[OC/EC]_{prim}$  is deemed constant, despite the reality that it may change  
 253 throughout the day depending on factors such as wind direction and the location of the dominant emission sources. Our 23-h  
 254 sampling is expected to smooth this variability source out; 2) It neglects  $OC_{prim}$  from non-combustion sources; and 3) It assumes  
 255 that  $OC_{prim}$  is nonvolatile and nonreactive. Departure from these assumptions implies that the estimation of  $OC_{prim}$  and  $OC_{sec}$   
 256 might be biased, likely underestimating  $OC_{sec}$ .

$$257 \quad OC_{prim} = [OC/EC]_{min} * EC + b \quad \text{Eq (2)}$$

$$259 \quad OC_{sec} = OC - OC_{prim} \quad \text{Eq (3)}$$

260  $OC_{prim}$  was also estimated by using an organic tracers method from three sources significant in the CRV, namely fossil fuel  
 261 combustion ( $OC_{FF}$ ), biomass burning ( $OC_{BB}$ ), and vegetable detritus ( $OC_{det}$ ).  $OC_{FF}$ ,  $OC_{BB}$  and  $OC_{det}$  were estimated using a  
 262 fitted linear model by robust regression with a M estimator with bisquare function, which were find the coefficients X, Y and  
 263 Z to multiply the tracers concentrations of each source. The tracers used were the sum of the BghiP and IcdP for fossil fuel  
 264 ( $T_{FF}$ ); levoglucosan for biomass burning ( $T_{BB}$ ); and the sum of the highest molecular weight alkanes ( $C_{27} - C_{33}$ ) for vegetable  
 265 detritus ( $T_{det}$ ). The sum of each tracers multiply multiply by X, Y and Z, respectively, Eq (5).  $T_{FF}$ ,  $T_{BB}$  and  $T_{det}$  corresponding to  
 266  $OC_{prim}$  attributed to known sources present in CRV. Th substration of  $OC_{prim}$  attributed to OC total is named  $OC_{rest}$ , which  
 267 corresponding to another sources of OC primary and OC secondary.

$$268 \quad OC_{prim} = (T_{FF} * X) + (T_{BB} * Y) + (T_{det} * Z) \quad \text{Eq (4)}$$

$$269 \quad OC_{prim} = OC_{FF} + OC_{BB} + OC_{det} \quad \text{Eq (5)}$$

$$270 \quad OC_{rest} = OC - OC_{prim} \quad \text{Eq (6)}$$

271  
 272 According to Table 1, OM was estimated from OC using conversion factors  $f_1$  and  $f_2$  (Chow et al., 2015), which are dependent  
 273 on the OM oxidation level and the secondary organic aerosol formation and aging during transportation. Turpin and Lim  
 274 (2001a) recommended an OM/OC ratio of  $1.6 \pm 0.2$  for urban aerosols, and  $2.1 \pm 0.2$  for non-urban aerosols, values comparable

Con formato: Subíndice

Con formato: Sin Resaltar

Con formato: Fuente: (Predeterminada) +Títulos (Times New Roman), Sin Superíndice / Subíndice

Con formato: Resaltar

Con formato: Resaltar

Con formato: Resaltar

Con formato: Resaltar

Con formato: Resaltar

Con formato: Resaltar

Con formato: Resaltar

Con formato: Resaltar

Con formato: Resaltar

Con formato: Resaltar

Con formato: Resaltar

Con formato: Resaltar

Con formato: Resaltar

Con formato: Resaltar

Con formato: Resaltar

Con formato: Resaltar

Con formato: Resaltar

Con formato: Resaltar

Con formato: Resaltar

Con formato: Resaltar

Con formato: Resaltar

Con formato: Resaltar

Con formato: Resaltar

Con formato: Resaltar

Con formato: Resaltar

Con formato: Resaltar

Con formato: Resaltar

Con formato: Resaltar

Con formato: Resaltar

Con formato: Resaltar

Con formato: Resaltar

Con formato: Fuente: Sin Cursiva

Con formato: Subíndice

Con formato: Fuente: Sin Cursiva

Con formato: Normal, No ajustar espacio entre texto latino y asiático, No ajustar espacio entre texto asiático y números

275 with those found by Aiken et al. (2008), of 1.71 (1.41 – 2.15), where lower values (1.6 – 1.8) are attributed to ground  
 276 measurements in the morning, and higher values (1.8 – 1.9) to aircraft sample measurements. BB aerosols can have even higher  
 277  $f$  values (2.2-2.6), due to the presence of organic components with higher molecular weights, e.g., levoglucosan. However,  
 278 Andreae (2019) recommends a factor of 1.6 for fresh BB aerosol, which is consistent with Hodshire et al (2019). We believe  
 279 that traffic and biomass burning are the dominant OC<sub>prim</sub> sources at our site. Therefore, we used  $f_{OC} = 1.6$  to estimate OM<sub>prim</sub>.  
 280 We used a factor of 2.1 to estimate OM<sub>sec</sub> from the OC<sub>sec</sub> fraction. This factor was chosen based on recommended ratios of  
 281 2.1±0.2 for aged aerosols (Schauer, 1998). Some of the global climate models used to estimate direct radiative forcing from  
 282 organic material present in the aerosols employ OM/OC ratios without separating the sources, while others change the ratio  
 283 depending on type of source using values ranging from 1.4 - 1.6 for fossil fuel and biofuel, and 2.6 for biomass burning. Other  
 284 set of models use specific molecules as tracers to follow the OM, such as monoterpenes, isoprene, aromatics and alkanes.  
 285 (Tsigaridis et al., (2014) present a list of tracers than haven been used in various models to quantify OM in the aerosols.

286 ▲  
 287 Concentration ratios among distinct species were used to chemically characterize and infer the main sources of fine particle  
 288 matter at Palmira. As a preliminary proxy for PM<sub>2.5</sub> acidity, the cation/anion equivalent ratio and the [NH<sub>4</sub><sup>+</sup>]/[SO<sub>4</sub><sup>2-</sup>] molar  
 289 ratio were used. The first one is based on electroneutrality and assumes that H<sup>+</sup> balances the excess of anions in the solution  
 290 considered, and the second one ratio is an indicator of acidity attributable to those two ions, which are usually the most  
 291 abundant cation and anion contained in the PM<sub>2.5</sub>. The cation equivalent to anion equivalent ratio was calculated using Eq (74)  
 292 and Eq (85) for each term.

293  
 294 However, these approaches to inferring the PM<sub>2.5</sub> acidity can result in challenging interpretations, incomplete and incorrect  
 295 results due to an indirect connection to the system's acidity (Pye et al., 2020). Therefore, the E-AIM (Extended Aerosol  
 296 Inorganics Model) was used to determine the equilibrium state of a system containing water and the following ions: SO<sub>4</sub><sup>2-</sup>,  
 297 NH<sub>4</sub><sup>+</sup>, NO<sub>3</sub><sup>-</sup>, Na<sup>+</sup> and Cl<sup>-</sup>, with an atmosphere of known temperature and relative humidity, without information on gas-phase  
 298 concentrations (NH<sub>3</sub>, HNO<sub>3</sub> and SO<sub>2</sub>), which were not available in this study. The H<sup>+</sup> mole fraction concentration from E-AIM  
 299 IV (Frieze and Ebel, 2010), was used to calculate pH following Eq (96). E-AIM requires that the input data for ionic  
 300 composition be balanced on an equivalent basis, which means that the sums of the charges on the cations and anions considered  
 301 in the system do balance, accordingly [SO<sub>4</sub><sup>2-</sup>] + [NO<sub>3</sub><sup>-</sup>] + [Cl<sup>-</sup>] = [NH<sub>4</sub><sup>+</sup>] + [Na<sup>+</sup>]. The disadvantage of this approach is that it  
 302 does not allow for the partitioning of trace gases into the vapor phase. The model is available to run on the following website:  
 303 <http://www.aim.env.uea.ac.uk/aim/model4/model4a.php> (last access: 22 January 2022).

304

$$305 \quad AE = \frac{[SO_4^{2-}]}{48} + \frac{[NO_3^-]}{62} + \frac{[C_2O_4^{2-}]}{44} + \frac{[Cl^-]}{35} + \frac{[PO_4^{3-}]}{31.3} + \frac{[NO_2^-]}{46} + \frac{[Br^-]}{79.9} + \frac{[F^-]}{18.9} + \frac{[CH_3O_3S^-]}{95} + \frac{[CHO_2^-]}{45} \quad \text{Eq (78)}$$

$$306 \quad CE = \frac{[Na^+]}{23} + \frac{[K^+]}{39} + \frac{[NH_4^+]}{18} + \frac{[Mg^{2+}]}{12} + \frac{[Ca^{2+}]}{20} \quad \text{Eq (89)}$$

Con formato: Fuente: Sin Cursiva

Con formato: Sin Superíndice / Subíndice

Con formato: Fuente: Sin Cursiva

Con formato

Con formato: Sin Superíndice / Subíndice

Con formato: Sin Superíndice / Subíndice

Con formato: Sin Superíndice / Subíndice

Con formato: Sin Tachado, Sin Resaltar

$$pH_x = -\log_{10}(He_{H\pm}^{*+}) \quad \text{Eq (9+9)}$$

Parent PAH ratios are widely used to identify combustion-derived PAHs (Khedidji et al., 2020; Szabó et al., 2015; Tobiszewski and Namieśnik, 2012), although some of them are photochemically degraded in the atmosphere (Yunker et al., 2002). Additionally, n-alkanes are employed as markers of fossil fuel or vegetation contributions to PM<sub>2.5</sub>. Carbon number maximum concentration (C<sub>max</sub>), carbon preference index (CPI), and wax n-alkanes percentage (WNA%) were the criteria utilized to determine the n-alkane origin. Table 2 summarizes the diagnostic ratio equations and the expected dominating source based on the ratio value.

Table 2. Diagnostic ratios of organic compounds used to infer the sources of PM<sub>2.5</sub> in this study.

Diagnostic ratios	Equation	Value	Source	References
BeP/(BeP+BaP)		<0.5 >0.5	Fresh particles Photolysis	(Tobiszewski and Namieśnik, 2012)
IcdP/(IcdP+BghiP)		<0.2 0.2 - 0.5 >0.5	Petrogenic Petroleum combustion Grass, wood and coal combustion	(Yunker et al., 2002) (Tobiszewski and Namieśnik, 2012)
BaP/BghiP		<0.6 >0.6	Non-traffic emissions Traffic emissions	(Tobiszewski and Namieśnik, 2012) (Szabó et al., 2015)
IcdP/BghiP		>1.25 <0.4	Brown coal* Gasoline	(Ravindra et al., 2008)
LMW/(MMW+HMW)		<1 >1	Pyrogenic Petrogenic	(Tobiszewski and Namieśnik, 2012)
C <sub>max</sub>		< C <sub>25</sub> C <sub>27</sub> - C <sub>34</sub>	Anthropogenic Vegetative detritus	(Lin et al., 2010)
CPI	$CPI = 0.5 * \left[ \frac{\sum_{20}^{33} C_i}{\sum_{20}^{32} C_k} + \frac{\sum_{22}^{33} C_l}{\sum_{22}^{34} C_k} \right]$	CPI ~1 CPI > 1	Fossil carbon Biogenic	(Marzi et al., 1993) (Kang et al., 2018)
WNA%	$\sum WNA_{C_n} = [C_n] - \left[ \frac{(C_{n+1}) + (C_{n-1})}{2} \right]$ $WNA\% = \frac{\sum WNA_{C_n}}{\sum Total\ n - alkanes}$ $PNA\% = 100 - WNA\%$	WNA ~ 100 PNA ~ 100	Biogenic Anthropogenic	(Lyu et al., 2019)

\*Used for residential heating and industrial operation.

As all measured variables were subject to analytical uncertainty and temporal variability, linear fitting parameters were obtained from Deming regressions as recommended for atmospheric measurements (Wu and Zhen Yu, 2018). The Spearman coefficient was selected instead of Pearson's as an indicator of statistical correlation between chemical components to reduce

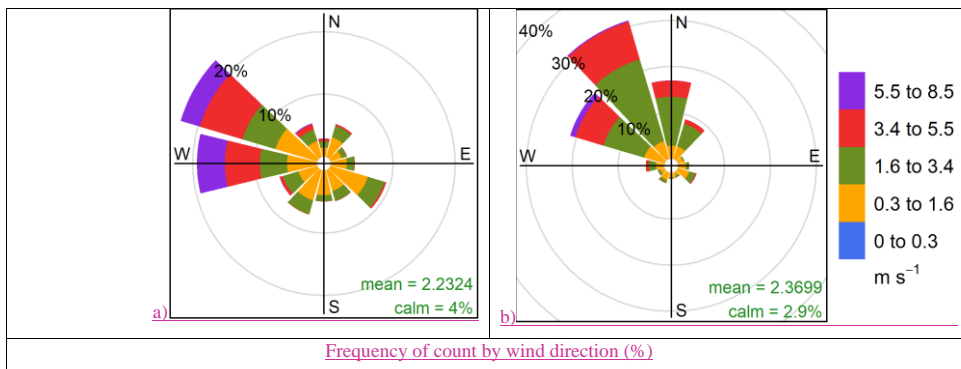
322 the effect of outliers. Derived ratios and other parameters were considered statistically significant when p-values < 0.05. The  
 323 statistical analysis was conducted using R version 4.0.2, 24 including the packages corr (0.4.2), mcr (1.2.1), cluster (2.1.0),  
 324 tidyverse (1.3.0), ggplot (3.3.2), MASS (7.3-53.1) and openair (2.7-4).

### 325 3. Results and discussions

#### 326 3.1. Meteorology

327

328 One year prior to the sampling period, we monitored the local meteorology, first at 14.5 m above the ground, a few meters  
 329 over the mean canopy level, and then at 32.5 m above the ground during the sampling campaign. The box-and-whisker plot in  
 330 Fig 2 shows katabatic tide winds of up to ~8 m/s at the sampling site elevation, peaking at ~17:00 LT. Wind speeds were a  
 331 factor ~2-3 slower at ground level. The wind runs at the sampling height were typically above ~200 km per day (Fig S3)  
 332 indicating that the samples had substantially broader spatial coverage of the CRV, much larger than it would have been at  
 333 ground level. This also implies that the samples were frequently and significantly influenced by emissions coming from  
 334 Yumbo's industrial hub (northwest of Palmira), and also by Palmira and Yumbo urban and highway emissions, as well as  
 335 sugarcane PHB and sugarcane mill emissions. The wind rose (Fig 2a) suggests that the influence of urban emissions from Cali,  
 336 CRV's largest city by far, was minor. Other meteorological variables are reported in the Supplementary Material (SM) (Fig  
 337 S2). Temperature (24.2°C on average) and relative humidity (71.6%) were very likely controlled by solar radiation (350 W m<sup>-2</sup>  
 338 on average). The late-afternoon katabatic tide is fast enough to temporarily reduce temperature. The daily pressure profile  
 339 (~763 hPa on average) clearly showed the influence of the katabatic tide, with a ~3 hPa drop during its arrival in the late  
 340 afternoon. Overall, we believe our measurements at the Palmira site are reasonably representative of the regional air quality.

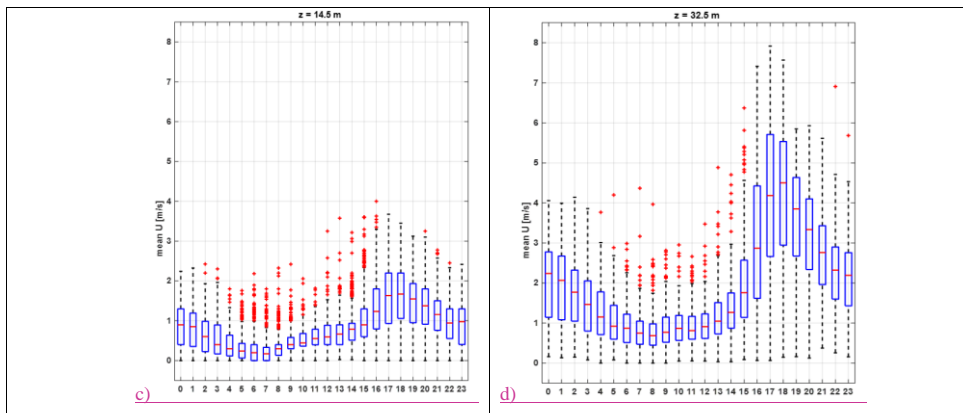


Frequency of count by wind direction (%)

Con formato: Derecha, Sangría: Izquierda: 0,63 cm

Tabla con formato

Con formato: Centrado



Con formato: Derecha

Con formato: Izquierda

341

342 Figure 2. Wind pattern in the sampling location: a) predominant wind rose during the sampling period (July - September  
 343 2018), b) hourly profile of wind speed at 14.5 m above the ground (August – December 2017), and c) hourly profile of wind  
 344 speed in sampling location at 32.5 m over the ground level (December 2017 – September 2018). \*Red points corresponding  
 345 to upper outliers of 10% outliers.  
 346

Con formato: Fuente: Sin Negrita

Con formato: Normal

### 347 3.2. Bulk $PM_{2.5}$ concentration and composition

348

349 The daily  $PM_{2.5}$  concentration measured in this study ranged from 6.73 to 24.45  $\mu\text{g m}^{-3}$  with a campaign average of  $14.38 \pm$   
 350  $4.35 \mu\text{g m}^{-3}$  (23 h-average,  $\pm 1$ -sigma). Although these concentrations may appear comparatively low, it is worth stressing that  
 351 samples were collected at more than 30 m height, with hourly wind speeds frequently above 4  $\text{m s}^{-1}$ . However, most days  
 352 during this study,  $PM_{2.5}$  concentration exceeded the 5  $\mu\text{g m}^{-3}$  annual mean and 15  $\mu\text{g m}^{-3}$  24-h mean guidelines by World Health  
 353 Organization, (2021). Nevertheless, the Colombian standards are less demanding, thus observed concentrations comply with  
 354 the 37  $\mu\text{g m}^{-3}$  24-h mean (MADS, 2017).  
 355

356

357 Previous studies conducted in rural areas of Brazil impacted by open field sugarcane burning reported significantly higher  
 358 (mean 22.7  $\mu\text{g m}^{-3}$ ; Lara et al., 2005), similar (mean 18  $\mu\text{g m}^{-3}$  Souza et al., 2014), and significantly lower  $PM_{2.5}$  concentrations  
 359 (mean 10.88  $\mu\text{g m}^{-3}$ ; Franzin et al., 2020). Comparable measurements in Mexico during harvest periods showed much higher  
 360 concentrations, from 29.14  $\mu\text{g m}^{-3}$  (Mugica-Alvarez et al., 2015) up to 51.3  $\mu\text{g m}^{-3}$  (Mugica-Álvarez et al., 2016). Our  $PM_{2.5}$   
 361 concentration measurements in the CRV are thus substantially lower than those usually reported in Mexico and Brazil during  
 362 sugarcane burning periods. Major differences among sugarcane PHB practices in Colombia, Brazil and Mexico must be  
 considered while comparing concentrations. First,  $\sim 1/3$  of the sugarcane harvested area is burned before harvest at CRV. This

363 fraction is much larger in Mexico and Brazil (FAO, 2020). Second, sugarcane is harvested year-round in CRV, as opposed to  
 364 Brazil and Mexico, where harvest is limited to a ~6-month period (known in Spanish as *zafra*, “the harvest”). Third, the size  
 365 of the individual plots burned in CRV is typically ~6 ha (median burned area; Cardozo-Valencia et al., 2019), compared to  
 366 much larger plots and total areas in Brazil and Mexico (FAO, 2020).

367

368 OC was the most abundant measured PM<sub>2.5</sub> component with a mean daily concentration of  $3.97 \pm 1.31 \mu\text{g m}^{-3}$ , whereas the  
 369 mean EC concentration was only  $0.96 \pm 0.31 \mu\text{g m}^{-3}$ . These two components contributed to  $29.1 \pm 8.3\%$  and  $7.2 \pm 2.3\%$  of the  
 370 PM<sub>2.5</sub> mass, respectively (carbonaceous fractions were thus  $4.93 \pm 1.58 \mu\text{g m}^{-3}$ , i.e.  $36.31 \pm 10.41\%$  of PM<sub>2.5</sub>).

371

372 The most abundant water-soluble ions found in Palmira’s PM<sub>2.5</sub> were SO<sub>4</sub><sup>2-</sup>, NH<sub>4</sub><sup>+</sup>, and NO<sub>3</sub><sup>-</sup>, with average concentrations of  
 373  $2.15 \pm 1.39 \mu\text{g m}^{-3}$ ,  $0.67 \pm 0.62 \mu\text{g m}^{-3}$ , and  $0.51 \pm 0.30 \mu\text{g m}^{-3}$ , respectively ( $12.7 \pm 2.8\%$ ,  $3.7 \pm 1.1\%$  and  $2.6 \pm 1.3\%$  of mass  
 374 concentration, respectively). Other water-soluble ions, such as Na<sup>+</sup>, Ca<sup>+</sup>, and C<sub>2</sub>O<sub>4</sub><sup>2-</sup>, had mean concentrations of around 0.1  
 375  $\mu\text{g m}^{-3}$ , while those of K<sup>+</sup>, PO<sub>4</sub><sup>3-</sup>, CH<sub>3</sub>O<sub>3</sub>S<sup>-</sup>, Mg<sup>2+</sup>, and Cl<sup>-</sup> had concentrations ranging from 10-80 ng m<sup>-3</sup> (Table 3Table-3).

376

377 The predominant elements were Ca ( $0.42 \pm 0.33 \mu\text{g m}^{-3}$ ), K ( $0.13 \pm 0.08 \mu\text{g m}^{-3}$ ), and Fe ( $88 \pm 65 \text{ ng m}^{-3}$ ), followed by Zn ( $34$   
 378  $\pm 33 \text{ ng m}^{-3}$ ), Pb ( $18 \pm 19 \text{ ng m}^{-3}$ ), Sn ( $52 \pm 37 \text{ ng m}^{-3}$ ), Ti ( $5 \pm 4 \text{ ng m}^{-3}$ ), Ba ( $9 \pm 13 \text{ ng m}^{-3}$ ), Sr ( $2 \pm 5 \text{ ng m}^{-3}$ ). Mn, Ni, Cr, and  
 379 Se concentrations were below  $2 \pm 1 \text{ ng m}^{-3}$ . Trace metals such as Ti, Cr, Mn, K, Ca, Fe, Ni, Cu, Zn Sr, Pb and Se were found  
 380 in all PM<sub>2.5</sub> samples, while V was found only in a few samples. Other trace metals such as As and Sb were detected only at a  
 381 reduced number of samples with concentrations below  $20 \text{ ng m}^{-3}$ . Table 3Table-3 shows the mean, standard deviation,  
 382 minimum, and maximum concentration of the carbonaceous fraction, soluble ions, and metals found in the PM<sub>2.5</sub> samples  
 383 collected in the CRV.

384

385 Table 3. Mean, 1 standard deviation, minimum and maximum concentrations of carbonaceous fraction, soluble ions, and  
 386 metals in samples of PM<sub>2.5</sub> collected in Palmira.

Species	# of samples	Mean	SD	Min	Max	Units
PM <sub>2.5</sub>	22	14.38	4.35	6.73	24.45	$\mu\text{g m}^{-3}$
OC	45	3.97	1.31	2.31	8.35	
EC	45	0.96	0.31	0.52	2.15	
SO <sub>4</sub> <sup>2-</sup>	45	2.15	1.39	0.98	10.27	
NH <sub>4</sub> <sup>+</sup>	45	0.67	0.62	0.18	4.29	
NO <sub>3</sub> <sup>-</sup>	45	0.51	0.30	0.11	1.45	
Na <sup>+</sup>	19	0.21	0.16	0.02	0.45	
Ca <sup>2+</sup> (Water soluble ion)	45	0.14	0.06	0.06	0.28	

C <sub>2</sub> O <sub>4</sub> <sup>2-</sup>	45	0.11	0.06	0.04	0.36
K <sup>+</sup> (Water soluble ion)	45	0.09	0.06	0.02	0.30
Ca <sup>2+</sup> (Trace metal)	42	0.42	0.33	0.01	1.95
K <sup>+</sup> (Trace metal)	43	0.13	0.08	0.02	0.46
Formate	13	82	88	0	217 ng m <sup>-3</sup>
PO <sub>4</sub> <sup>3-</sup>	21	66	42	10	148 worldwide
Methansulfonate	45	50	36	13	256
Cl <sup>-</sup>	30	20	19	0	75
Mg <sup>+2</sup>	45	19	10	2	52
NO <sub>2</sub> <sup>-</sup>	45	3	1	1	6
Fe	42	88	64	2	293
Sn	23	52	37	9	137
Zn	42	34	33	0	153
Pb	42	18	19	0	84
Ba	20	9	13	2	72
Sb	19	8	5	3	22
Cu	42	6	5	1	22
Ti	42	5	4	0	17
As	5	2	4	0	10
Mn	42	2	1	0	5
Ni	42	2	1	0	9
Sr	42	2	5	0	28
Cr	41	1	1	0	4
Se	41	1	1	0	6
V	20	0	1	0	3

Con formato: Resaltar

387

### 388 3.3. Ions

389 SO<sub>4</sub><sup>2-</sup> and NH<sub>4</sub><sup>+</sup> were the most prevalent abundant anion and cation in the PM<sub>2.5</sub> samples. The SO<sub>4</sub><sup>2-</sup> and NH<sub>4</sub><sup>+</sup> were the most  
 390 abundant anion and cation in the PM<sub>2.5</sub> samples. The molar ratio of between these most abundant cation and anion  
 391 [NH<sub>4</sub><sup>+</sup>]/[SO<sub>4</sub><sup>2-</sup>] was 1.6 ± 0.3 (min: 0.8 and max: 2.3), suggesting that PM<sub>2.5</sub> is acid conditions in PM<sub>2.5</sub> can be inferred  
 392 because this molar ratio was less than two. Acidic conditions in PM<sub>2.5</sub> can be inferred, since this ratio was less than two. The  
 393 pH of the PM<sub>2.5</sub> samples was determined using the IV E-AIM thermodynamic model, in which estimates the activity  
 394 coefficient of these species in aqueous phase equilibrium was estimated using the H<sup>+</sup>-NH<sub>4</sub><sup>+</sup>-Na<sup>+</sup>-SO<sub>4</sub><sup>2-</sup>-NO<sub>3</sub><sup>-</sup>-Cl<sup>-</sup>-H<sub>2</sub>O system.  
 395 As a result, the pH of PM<sub>2.5</sub> samples collected in the CRV was constant enough, with a mean of 2.5 ± 0.4. The correlation  
 396 observed between the ratio [NH<sub>4</sub><sup>+</sup>]/[SO<sub>4</sub><sup>2-</sup>] and the pH was strong (r<sup>2</sup> = 0.96, as plot in Figure S3), showing suggesting that the  
 397 molar concentrations of those ions can explain significantly explain the particle acidity, assess the acidity of the PM<sub>2.5</sub> samples,  
 398 pH was calculated from of IV E-AIM thermodynamic model, in which the system conformed by H<sup>+</sup>-NH<sub>4</sub><sup>+</sup>-Na<sup>+</sup>-SO<sub>4</sub><sup>2-</sup>-NO<sub>3</sub><sup>-</sup>-



399  $\text{Cl}^-/\text{H}_2\text{O}$  was parametrized to estimate the activity coefficient of these species in aqueous phase equilibrium. As result, the pH  
 400 of  $\text{PM}_{2.5}$  samples collected in the CRV was constant enough, with a mean of  $2.5 \pm 0.4$ . The correlation observed between  
 401  $[\text{NH}_4^+]/[\text{SO}_4^{2-}]$  and pH was strong ( $r^2 = 0.96$ , as plot in Figure S3), which suggest that this molar ratio is a simple form to  
 402 follow the particles acidity in CRV. Other studies have found present similar values to  $[\text{NH}_4^+]/[\text{SO}_4^{2-}]$  molar ratio values for  
 403 pH values lower measured smaller than the estimated in CRV. For instance Xue et al., (2011), for example, shows molar  
 404 ratios in ranging from 1.32 to 1.71 and pH values between -0.45 to and 0.59. The estimation of particles To identify the  
 405 aerosols acidity in CRV help to understanding the mechanisms of processes of gas particle partitioning, acid catalytic  
 406 reactions and metal dissolution in the  $\text{PM}_{2.5}$  that happen in the aerosols observed in CRV (Pye et al., 2020). Pye et al., (2020)  
 407 showed that Fine particles show have a bimodal distribution of pH, with onea population of particles having a one mode  
 408 around mean a pH of 1-3, and another mode around a pH of 4-5, the latter population, influenced by dust, sea spray, and  
 409 potentially biomass burning, having an average pH closer to 4-5 (Pye et al., 2020). In this study, only just one  $\text{PM}_{2.5}$  sample  
 410 exceed a pH value of 4. Overall, this is an indicator of the abundance of sulfate and organics compounds in samples collected  
 411 in the CVR.

412

413 The pH affects the partitioning of total nitrate ( $\text{NO}_3^- + \text{HNO}_3$ ) and total ammonium ( $\text{NH}_4^+ + \text{NH}_3$ ) between the gas and  
 414 particulate phases. Lower pH values favor the partitioning of total nitrate toward the gaseous phase ( $\text{HNO}_3$ ) rather than the  
 415 particulate phase ( $\text{NO}_3^-$ ). In contrast, the partitioning of total ammonium is favored toward the particulate phase, remaining as  
 416  $\text{NH}_4^+$  over in the aerosol, whereas  $\text{SO}_4^{2-}$  is a nonvolatile species that remained in the particulate phase. Acidity conditions in  
 417 the samples collected in this study are consistent with concentrations of  $\text{SO}_4^{2-}$ ,  $\text{NH}_4^+$ , and  $\text{NO}_3^-$ , corresponding to  $2.5 \mu\text{g m}^{-3}$ ,  
 418  $0.7 \mu\text{g m}^{-3}$ , and  $0.5 \mu\text{g m}^{-3}$ , respectively. Ammoniated sulfate and ammonium nitrate are generally considered the predominant  
 419 forms of nitrate and sulfate in the inorganic fraction in fine particles. In limited environmental ammonium conditions, ammonia  
 420 reacts preferentially with  $\text{H}_2\text{SO}_4$  to form ammonium sulfate ( $[\text{NH}_4]_2\text{SO}_4$ ), letovicite ( $[\text{NH}_4]_3\text{H}[\text{SO}_4]_2$ ) or ammonium bisulfate  
 421 ( $[\text{NH}_4\text{HSO}_4]$ ) (Lee et al., 2008). Although the correlation coefficient between  $\text{SO}_4^{2-}$  and  $\text{NH}_4^+$  concentrations was high ( $R^2 =$   
 422  $0.98$ ), the amount of ammonium contained in the samples was not high enough to neutralize sulfate completely and form  
 423  $[\text{NH}_4]_2\text{SO}_4$ . In environmental with limited concentrations of ammonium, is expected the formation of sulfate salts not  
 424 completely neutralized, as  $[\text{NH}_4]_3\text{H}[\text{SO}_4]_2$  and  $[\text{NH}_4\text{HSO}_4]$  (Ianniello et al., 2011). Thus, based on the limited ammonium  
 425 concentrations found in  $\text{PM}_{2.5}$  of CRV, the stoichiometric molar ratio between  $[\text{NH}_4^+]/[\text{SO}_4^{2-}]$  of 3:2 for letovicite and 1:1 for  
 426 ammonium bisulfate, and the results of the E-AIM model, it is possible to indicate that there is a mixture of sulfate salts, such  
 427 as, ammonium bisulfate, letovicite, and ammonium sulfate, which is going to form progressively, according to ammonia  
 428 availability. The E-AIM model presents the saturation ratio of each solid species, which usually forms before ammonium  
 429 bisulfate than letovicite and ammonium sulfate. For a molar ratio of 1.5, the aerosol phase consists almost exclusively of  
 430 letovicite and to form ammonium sulfate, the ratio should be over 2.0 (Seinfeld and Pandis, 2006). As result of the

431 [\[NH<sub>4</sub><sup>+</sup>\]/\[SO<sub>4</sub><sup>2-</sup>\]](#) ratios observed in the samples collected in CRV and the pH estimated from the IV E-AIM model, there is no  
 432 [reason to assume that nitrate is present as ammonium nitrate in the PM<sub>2.5</sub>.](#)

433 [Therefore, there is no reason to assume that nitrate is present as ammonium nitrate.](#)

434  
 435 [Instead of this, NO<sub>3</sub><sup>-</sup> might be bound to cations contained in sea salt and dust particles to form relative nonvolatile salts, as](#)  
 436 [KNO<sub>3</sub>, NaNO<sub>3</sub> and Ca\(NO<sub>3</sub>\)<sub>2</sub>. NO<sub>3</sub><sup>-</sup> showed correlation with Na<sup>+</sup>, Ca<sup>2+</sup> and K<sup>+</sup> \(r<sup>2</sup> = 0.6, 0.2 and 0.2, respectively\), indicating](#)  
 437 [possible formation of those salts. The correlation between Na<sup>+</sup> and NO<sub>3</sub><sup>-</sup> could be explained by the impact of sea salt aerosol](#)  
 438 [that comes from air mass origin in the Pacific Ocean. However, the amount of Na<sup>+</sup> is not enough to neutralize the total of NO<sub>3</sub><sup>-</sup>](#)  
 439 [, while Ca<sup>2+</sup> showed to be enough amount to neutralize the NO<sub>3</sub><sup>-</sup>. The molar ratio observed in PM<sub>2.5</sub> samples of CRV for \[NO<sub>3</sub><sup>-</sup>](#)  
 440 [\]/\[Ca<sup>2+</sup>\] was 2.6 ± 1.4, \[NO<sub>3</sub><sup>-</sup>\]/\[Na<sup>+</sup>\] was 1.7 ± 1.3, and \[NO<sub>3</sub><sup>-</sup>\]/\[K<sup>+</sup>\] was 5.0 ± 3.2, overcoming the stoichiometric molar ratio](#)  
 441 [required to form Ca\(NO<sub>3</sub>\)<sub>2</sub>, NaNO<sub>3</sub>, and KNO<sub>3</sub>.](#)

442  
 443 [While, ~~In~~ this study, the abundance of SO<sub>4</sub><sup>2-</sup> in PM<sub>2.5</sub> can be attributed to oxidation of SO<sub>2</sub> and SO<sub>3</sub> emitted by from coal](#)  
 444 [fired in power plants and industrial facilities \(Wang et al., 2016\), biomass burning activities \(Song et al. \(2006\)\) and the](#)  
 445 [emission of H<sub>2</sub>S in poultry production \(Casey et al., 2006\). The H<sub>2</sub>S emission from poultry and pork production is estimated](#)  
 446 [using the factor emission given by animal units \(AU\) and the time that it stays in the housing, where one AU corresponding to](#)  
 447 [500 Kg of body mass. H<sub>2</sub>S emissions from swine and poultry housing trend to be under 5 g H<sub>2</sub>S AU<sup>-1</sup> d<sup>-1</sup> Casey et al., \(2006\),](#)  
 448 [which can reach a 3.5 Ton H<sub>2</sub>S d<sup>-1</sup> by poultry and 5 Ton H<sub>2</sub>S d<sup>-1</sup> by pork production. Ammonia emissions factors by poultry](#)  
 449 [and livestock vary from 0.09 to 12.9 AU<sup>-1</sup> d<sup>-1</sup> which represents 9.05 Ton NH<sub>3</sub> d<sup>-1</sup> by poultry housing and 12. Ton d<sup>-1</sup> by pork](#)  
 450 [production.](#)

451  
 452 [PM<sub>2.5</sub> consistently contained methanesulfonate, with an average concentration of 50 ng ± 13 m<sup>-3</sup>. This ion is produced by the](#)  
 453 [aqueous oxidation of dimethyl sulfide \(DMS\), one of the most prevalent biogenic sulfur compounds in the troposphere. DMS](#)  
 454 [oxidation is a major source of non-sea salt sulfate aerosols in marine areas \(Tang et al., 2019\), but also can have origin in](#)  
 455 [continental origins, such as biomass burning, \(Gondwe, 2004; Meinardi et al., 2003; Sorooshian et al., 2015; Stahl et al., 2020\).](#)  
 456 [Methanesulfonate was mainly correlated to the ions sulphate and ammonia \(r<sup>2</sup> = 0.88\) and C<sub>2</sub>O<sub>4</sub><sup>2-</sup> \(r<sup>2</sup> = 0.66\), the metals Se \(r<sup>2</sup>](#)  
 457 [= 0.74\) and Fe \(r<sup>2</sup> = 0.41\) and the carbonaceous fraction EC \(r<sup>2</sup> = 0.56\) and OC \(r<sup>2</sup> = 0.49\) in this study. Knowing the origin](#)  
 458 [of this ion in PM<sub>2.5</sub> in CRV, which is not directly coastal area, prompts future studies with a higher time resolution \(6-12](#)  
 459 [hours\) to establish the connection with changes in the wind pattern and the impact of the katabatic circulation, especially](#)  
 460 [because biomass burning, mainly from sugarcane burnt, is an activity developing during all year in CRV.](#)

461 [In ammonia limited situations, NO<sub>3</sub><sup>-</sup> might be bound to cations contained in sea salt and dust particles to form relative](#)  
 462 [nonvolatile salts, as KNO<sub>3</sub>, NaNO<sub>3</sub> and Ca\(NO<sub>3</sub>\)<sub>2</sub>. NO<sub>3</sub><sup>-</sup> showed correlation with Na<sup>+</sup>, Ca<sup>2+</sup> and K<sup>+</sup> \(r<sup>2</sup> = 0.6, 0.2 and 0.2,](#)  
 463 [respectively\), indicating possible formation of those salts. The correlation between Na<sup>+</sup> and NO<sub>3</sub><sup>-</sup> could be explained by the](#)

464 impact of sea salt aerosol that comes from air mass origin in the Pacific Ocean. However, the amount of  $\text{Na}^+$  is not enough to  
 465 neutralize the total of  $\text{NO}_3^-$ , while  $\text{Ca}^{2+}$  showed to be enough amount to neutralize the  $\text{NO}_3^-$ . The molar ratio observed in  $\text{PM}_{2.5}$   
 466 samples of CRV for  $[\text{NO}_3^-]/[\text{Ca}^{2+}]$  was  $2.6 \pm 1.4$ ,  $[\text{NO}_3^-]/[\text{Na}^+]$  was  $1.7 \pm 1.3$ , and  $[\text{NO}_3^-]/[\text{K}^+]$  was  $5.0 \pm 3.2$ , overcoming the  
 467 stoichiometric molar ratio required to form  $\text{Ca}(\text{NO}_3)_2$ ,  $\text{NaNO}_3$ , and  $\text{KNO}_3$ .

468  
 469 Methanesulfonate is produced predominantly by aqueous oxidation of dimethyl sulfide (DMS), one of the most abundant  
 470 biogenic sulfur compounds in the troposphere. The oxidation of DMS is an important source of non-sea salt sulfate aerosol in  
 471 marine regions (Tang et al., 2019), but can also have terrestrial sources, including biomass burning (Gondwe, 2004; Meinardi  
 472 et al., 2003; Sorooshian et al., 2015; Stahl et al., 2020).  $\text{C}_2\text{O}_4^{2-}$  ( $r^2 = 0.66$ )  $\text{C}_2\text{O}_4^{2-}$  Future studies with a higher time resolution (6  
 473 –12 hours)

474 Methanesulfonate is produced predominantly by aqueous oxidation of dimethyl sulfide (DMS), one of the most abundant  
 475 biogenic sulfur compounds in the troposphere. The oxidation of DMS is an important source of non-sea salt sulfate aerosol in  
 476 marine and oceanic regions (Tang et al., 2019), but can also have terrestrial sources, including biomass burning (Gondwe,  
 477 2004; Meinardi et al., 2003; Sorooshian et al., 2015; Stahl et al., 2020) (Gondwe 2004, sorooshian 2015). Methanesulfonate is  
 478 an organosulfur (OS) compound that can potentially impact the hygroscopicity and surface tension of particles and are useful  
 479 tracers for secondary aerosol formation (SOA) (Sorooshian et al., 2015). This ion is one of the most easily measured OS species  
 480 and its concentration can be used as a way of estimating the contribution of biogenic emissions on total sulfate levels. In  
 481 addition to the oceanic source, methanesulfonate also has terrestrial sources, such as wetlands, freshwater lakes, alfalfa,  
 482 ruminants, biomass burning, urban and agriculture emissions (Gondwe, 2004; Sorooshian et al., 2015). The  
 483  $[\text{methanesulfonate}]/[\text{SO}_4^{2-}]$  ratio can be used to infer the origin of its compound and distinguish the impact of fires in the  
 484 aerosols (Sorooshian et al., 2015) (sorooshian, 2015). In this study the  $[\text{methanesulfonate}]/[\text{SO}_4^{2-}]$  ratio was  $0.02 \pm 0.06$  (min:  
 485 0.012 – max: 0.03), suggesting a minor impact of biogenic sulfur compared to the total inorganic sulfate concentration.  
 486 However, the correlation between these two ions was very strong ( $r^2 = 0.88$ ). This can be indicative of the existence of OS  
 487 compounds, not included in this study, as part of the total sulfate levels. According to the average  $[\text{methanesulfonate}]/[\text{SO}_4^{2-}]$   
 488 ratios presented by Sorooshian et al., (2015), coastal regions exhibit higher values (0.06 to 0.09) than inland regions (0.02–  
 489 0.04). It is then possible to suppose that high methanesulfonate concentrations in the CRV were derived from continental  
 490 sources. This is supported by the non-existent correlation between  $\text{Na}^+$  and methanesulfonate, and the moderate correlation  
 491 between  $\text{C}_2\text{O}_4^{2-}$  and methanesulfonate ( $r^2 = 0.66$ ). Future studies with a higher time resolution (6 –12 hours) would be  
 492 necessary to confirm the contribution of biomass burning to methanesulfonate in the aerosol. Even though the air mass from  
 493 the Pacific Ocean has an impact on winds that ventilate the CRV in the late afternoon, the western mountain range may act as  
 494 a barrier for an important fraction of sea salt aerosol.

496 The measured average ratio of  $[\text{SO}_4^{2-}]/[\text{NO}_3^-] = 4.5 \pm 2.9$ . This ratio is higher than the one obtained by Souza et al. (2014) at  
497 Piracicaba ( $3.6 \pm 1.0$ ) and Sao Paulo ( $1.8 \pm 1.0$ ), Brazil. The strong correlations between  $\text{SO}_4^{2-}$  and  $\text{NH}_4^+$  ( $r^2 = 0.84$ ),  $\text{SO}_4^{2-}$  and  
498 methanesulfonate ( $\text{CH}_3\text{O}_3\text{S}^-$ ) ( $r^2 = 0.88$ ), and  $\text{SO}_4^{2-}$  and oxalate dianion ( $\text{C}_2\text{O}_4^{2-}$ ) ( $r^2 = 0.71$ ) allow us to infer that inorganic  
499 secondary aerosol formation is a significant  $\text{PM}_{2.5}$  source in the CRV. In addition, the presence of potassium cation ( $\text{K}^+$ ) in  
500 submicron particles is recognized as a biomass burning tracer (Andreae, 1983; Ryu et al., 2004).  $\text{K}^+$  showed a moderate  
501 correlation with nitrite anion ( $\text{NO}_2^-$ ) ( $r^2 = 0.44$ ) and  $\text{C}_2\text{O}_4^{2-}$  ( $r^2=0.43$ ) in the CRV, which suggests that biomass burning  
502 influences secondary aerosol formation.  $\text{Mg}^{2+}$  and  $\text{Ca}^{2+}$  ions, usually considered crustal metals, exhibited a moderate  
503 correlation of  $r^2 = 0.59$  (Li et al., 2013). Also,  $\text{Mg}^{2+}$  and  $\text{C}_2\text{O}_4^{2-}$  moderate correlation ( $r^2 = 0.26$ ) points to a link between crustal  
504 species and secondary aerosols. Such an association could be plausibly explained by soil erosion induced by pyro-convection  
505 during sugarcane pre-harvest burning (Wagner et al., 2018). Our study full species correlation matrix is shown in Fig 4S.  
506

#### 507 3.4. Metals

508  
509 The measured total  $\text{PM}_{2.5}$  trace metal concentration was  $706 \pm 462 \text{ ng m}^{-3}$  ( $101.3 \text{ ng m}^{-3}$  to  $2638 \text{ ng m}^{-3}$ ). Trace metals can  
510 originate from non-exhaust and exhaust emissions. Non-exhaust emissions come from brake and tire wear, road surface  
511 abrasion, wear/corrosion of other vehicle components, and the resuspension of road surface dust (Pant and Harrison, 2013).  
512 Metals in exhaust emissions are related to fuel, lubricant combustion, catalytic converters, and engine corrosion. As shown by  
513 Kundu and Stone (2014), many of these sources share some metals in their chemical composition profile, thus an unambiguous  
514 specific source attribution is non-trivial. In this study, we found a significant correlation among Fe, Mn and Ti ( $r^2 \approx 0.72$ ),  
515 which is typically associated with a high abundance of crustal material (Fomba et al., 2018), indicating that soil dust is a  
516 significant source in the CRV. Also, tire and brake wear tracer metals, including Zn and Cu, showed weaker but still significant  
517 correlations among them ( $r^2 \approx 0.32$ ). Ca concentrations were quite high ( $405 \pm 334 \text{ ng m}^{-3}$  ( $1.6 \text{ ng m}^{-3}$  to  $1952 \text{ ng m}^{-3}$ )). These  
518 levels can be attributed to dust generation by agricultural practices, particularly land planning, liming and tilling, PHB pyro-  
519 convection-induced soil erosion, and traffic-induced soil resuspension on unpaved rural roads. One of the very few previous  
520 investigations into on PM composition in the CRV (Criollo and Daza, 2011) analyzed trace metals in  $\text{PM}_{10}$  at 4 CRV locations,  
521 including Palmira. They found significant enrichment of Fe and K metals at locations exposed to PHB. It must be kept in mind  
522 that  $\text{PM}_{10}$  samples included coarse mode aerosols, of which dust might have been a significant fraction. Also, environmental  
523 regulations have been successful in steadily reducing the sugarcane burned area in the CRV since 2009. The Burned area  
524 dropped from 72% in 2011 to 35.46% in 2018, our year of measurements (Cardozo-Valencia et al., 2019).

525  
526 Cd, Pb, Ni, Hg and As, and other metals and metalloids are considered carcinogenic (WHO Regional Office for Europe, 2020).  
527 Measured concentrations of Pb and Ni in  $\text{PM}_{2.5}$  at Palmira were  $18 \text{ ng m}^{-3}$  (+/-19) and  $2 \text{ ng m}^{-3}$  (+/-1), respectively. These

528 mean values were below the EU target values of ( $0.5 \mu\text{g m}^{-3}$  and  $20 \text{ ng m}^{-3}$  respectively) (WHO, 2013a), and below the annual  
529 average limit of the Colombian national ambient air quality standard ( $0.5 \mu\text{g m}^{-3}$  and  $0.18 \mu\text{g m}^{-3}$  respectively) (MADS, 2017).  
530 Nevertheless, these concentrations are significantly higher than those reported for other suburban areas in Midwestern United  
531 States and remote sites in the northern tropical Atlantic (Fomba et al., 2018; Kundu and Stone, 2014). Pb concentrations are  
532 similar to those reported for Bogota and other large urban areas (SDA, 2010; Vasconcellos et al., 2007). Pb has been long  
533 banned as a fuel additive in Colombia, thus the observed levels might be associated with metallurgical industry and waste  
534 incineration. Information on ambient air hazardous metal concentrations in Latin America's urban and rural areas is still scarce.  
535

### 536 3.5. Carbohydrates

537

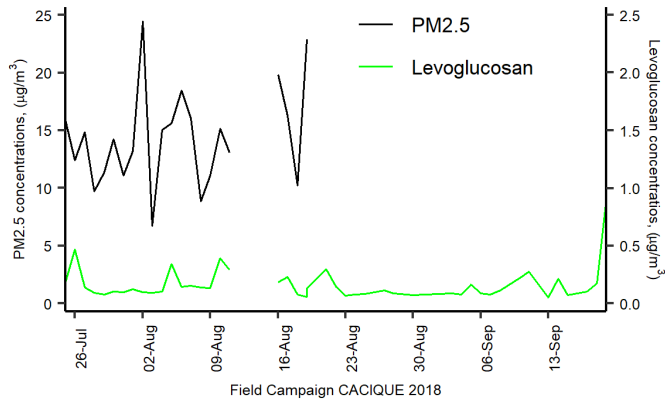
538 Levoglucosan is a highly specific biomass burning organic tracer (Bhattarai et al., 2019). Along with  $\text{K}^+$ , OC and EC, it can  
539 be used to effectively identify the relevance of biomass burning as an aerosol source. The relative contribution of levoglucosan  
540 to the PM carbohydrate burden, and especially the levoglucosan to mannosan ratio, can be used as indicators of the type of  
541 biomass burned (Engling et al., 2009). In this study, the following carbohydrates were quantified: levoglucosan, mannosan,  
542 glucose, galactosan, fructose and arabitol. Levoglucosan was by far the most abundant ( $113.8 \pm 147.2 \text{ ng m}^{-3}$ ), reaching values  
543 of up to  $904.3 \text{ ng m}^{-3}$ , followed by glucose ( $10.4 \pm 6.1 \text{ ng m}^{-3}$ ), mannosan ( $7 \pm 6.1 \text{ ng m}^{-3}$ ), and arabitol ( $4.1 \pm 3.5 \text{ ng m}^{-3}$ ).  
544 Levoglucosan and mannosan were detected in all  $\text{PM}_{2.5}$  samples, while galactosan and fructose were detected only in 9 and 11  
545 samples, respectively. Levoglucosan was  $3.5 \pm 2.3\%$  of OC and  $0.96\% \pm 0.81\%$  of  $\text{PM}_{2.5}$ .

546

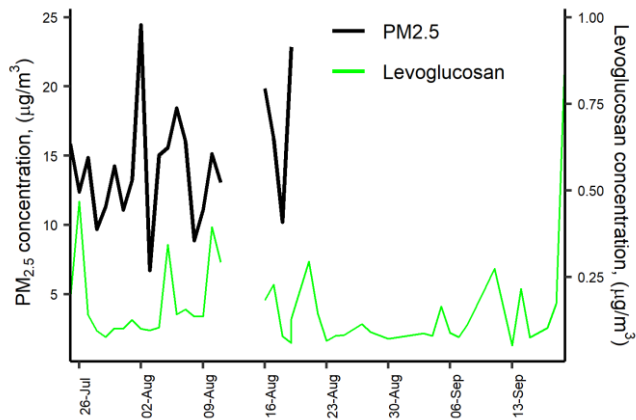
547 The levoglucosan concentration found in this study was quite similar to that reported in areas of Brazil where sugarcane  
548 production and processing are important economic activities, [Figure 3](#) ~~Figure-3~~. For instance, during the harvest (*zafra*) period  
549 in Araraquara, the levoglucosan mean concentration was  $138 \pm 91 \text{ ng m}^{-3}$ , although during the non-harvest period it was  
550 unexpectedly high ( $73 \pm 37 \text{ ng m}^{-3}$ ) (Urban et al., 2014). Likewise, the levoglucosan average concentration at Piracicaba during  
551 a reduced fire period was  $66 \text{ ng m}^{-3}$  (Souza et al., 2014). The measured mean levoglucosan/mannosan ratio in Palmira was  $17.6$   
552  $\pm 13.0$  (min: 8.1 – max: 58.1). Chemical profile studies found a levoglucosan/mannosan ratio of  $\sim 10$  for sugarcane leaves  
553 burned in stoves (Hall et al., 2012; Dos Santos et al., 2002) and of  $\sim 54$  for burned bagasse (Dos Santos et al., 2002). Leaves  
554 constitute the largest fraction (20.8%, Victoria et al., 2002) of pre-harvest burned sugarcane. Consistently and expectably, the  
555 levoglucosan/mannosan ratio at Palmira is much closer to the chemical profile ratio of leaves than that of bagasse. Moreover,  
556 ambient air samples in Araraquara and Piracicaba showed levoglucosan/mannosan ratios of  $9 \pm 5$  and  $\sim 33$ , respectively. For  
557 comparison, the levoglucosan/mannosan ratio in PM from rice straw and other crops burned were  $\sim 26.6$  and  $\sim 23.8$ , respectively  
558 (Engling et al., 2009). This indicates that the levoglucosan/mannosan ratio is sensitive to the type of biomass burned but also  
559 to burning conditions. The large levoglucosan/mannosan ratio in our study suggests that Palmira was impacted by sugarcane  
560 PHB most of the time, and, to a lesser extent, by bagasse combustion in sugar mills. We hypothesize that, even if these were

561 very small, levoglucosan and mannosan combustion emissions might not be negligible as the CRV sugarcane biomass yields  
 562 are very high and most of the harvested sugarcane bagasse is combusted for electric power and steam production.

563



564



565

566

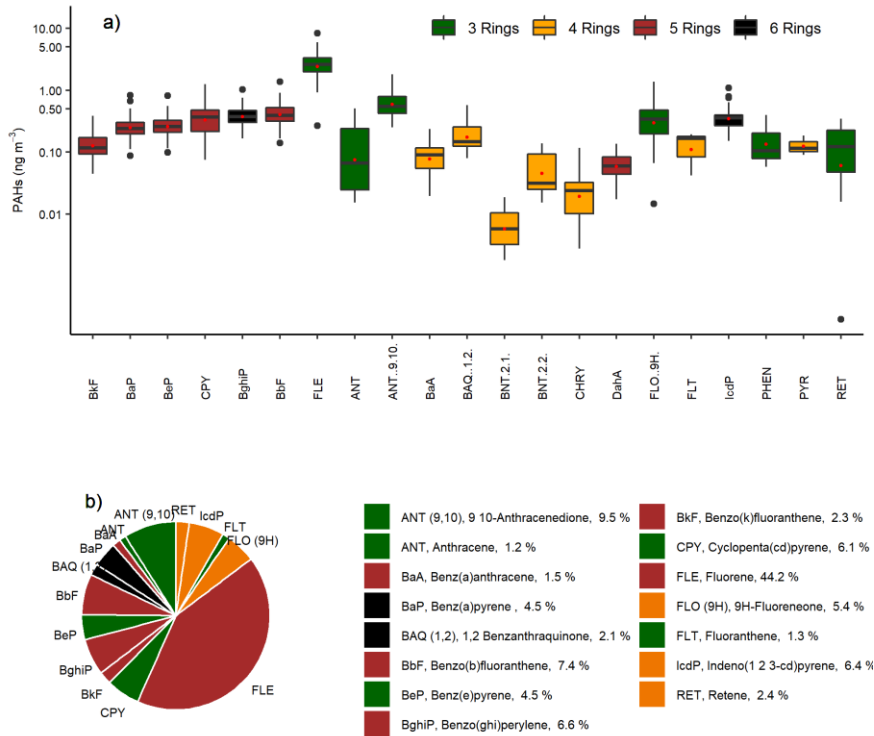
Figure 3. Daily variation of Levoglucosan and PM2.5 concentration at CRV.

567 **3.6. Polycyclic Aromatic Hydrocarbons (PAHs)**

568

569 A total of 22 PAHs were measured in each sample collected at Palmira, including the 16 PAHs listed as human health  
 570 priority pollutants by WHO and US-EPA (Yan et al., 2004). The total PAHs concentration was  $5.6 \pm 2.9 \text{ ng m}^{-3}$  (min:  $2.3 \text{ ng}$   
 571  $\text{m}^{-3}$  – max:  $15.8 \text{ ng m}^{-3}$ ).

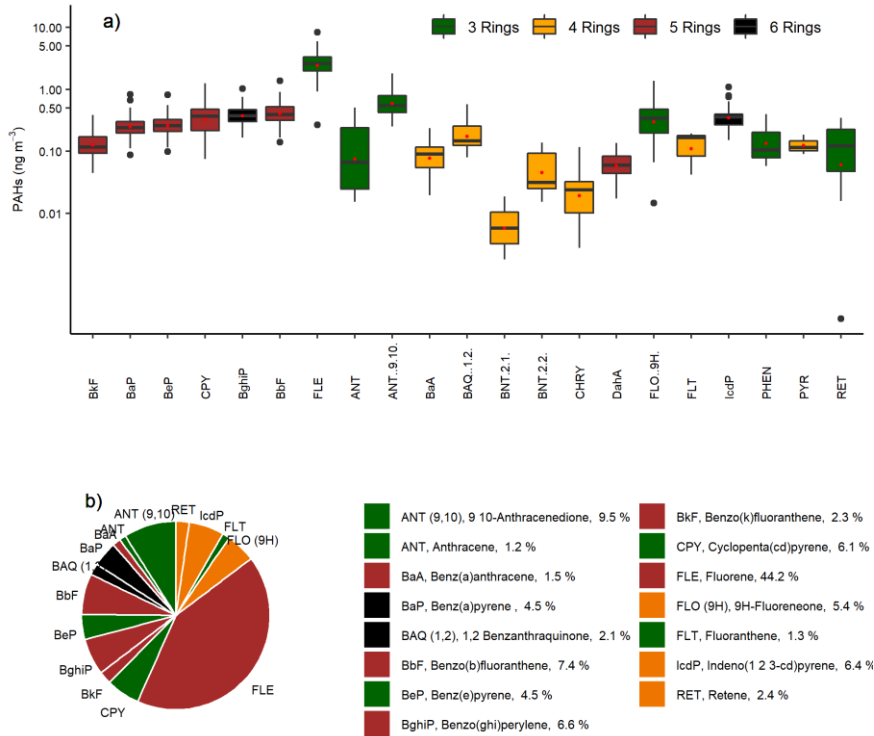
Con formato: Centrado



572

573 **Figure 4** Figure 4a shows the PAHs concentration variability during the sampling campaign (mean and standard deviation are  
 574 available in Table S2). The most abundant PAH were FLE (44.2%±11.9% total concentration share), ANT (9,10  
 575 (10.0%±4.5%), BbF (7.4%±2.3%), BghiP (6.7%±2.4%), IcdP (6.4%±1.9%), CPY (6.0%±2.3%), FLO (9H) (5.4%±3.1%),

BeP(4.6%±1.3%), and BaP(4.4%±1.6%), which accounted for 95.1% of the total PAH concentration (



578 [Figure 4](#)Figure 4b). Three-ring PAHs were the most abundant (59.04% of total PAH). Put together, five- and six-ring PAHs  
 579 accounted for an additional 38.44%. The less abundant PAH group was the four-ring (2.52%). A previous study in CRV,  
 580 carried out on PM<sub>10</sub> samples by Romero et al. (2013), showed higher FLT, PYR, and PHE concentrations in areas highly  
 581 exposed to sugarcane PHB compared to other locations. In contrast, PM<sub>2.5</sub> FLE concentrations in this research were  
 582 significantly higher than those in PM<sub>10</sub> by Romero et al. (2013), while PYR and PHE levels were similar.



584 The carcinogenic species BaP, BbF, BkF, BaA, BghiP, FLE, CPY and BeP were identified in all the PM<sub>2.5</sub> samples. BaP is a  
585 reference for PAH carcinogenicity (WHO, 2013a) that is used as a PAH exposure metric, known as the Benzo(a)Pyrene-  
586 equivalent carcinogenic potency (BaPE). We calculated BaPE using the toxic equivalent factors (TEF) proposed by Nisbet  
587 and LaGoy (1992) and (Malcolm and Dobson, 1994). PAH concentrations were multiplied by TEF and then added to estimate  
588 the carcinogenic potential of PM<sub>2.5</sub>-bounded PAHs. The mean carcinogenicity level at Palmira, expressed as BaP-TEQ, was  
589  $0.4 \pm 0.2 \text{ ng m}^{-3}$  (min:  $0.1 \text{ ng m}^{-3}$  - max:  $1.4 \text{ ng m}^{-3}$ ). Only one sample exceeded the Colombian annual limit of  $1 \text{ ng m}^{-3}$  but  
590 most of them exceeded the WHO reference level of  $0.12 \text{ ng m}^{-3}$ . The mutagenic potential of PAHs (BaP-MEQ) was estimated  
591 using the mutagenic equivalent factors (MEF) reported by Durant et al., (1996). The average BaP-MEQ was  $0.5 \pm 0.3 \text{ ng m}^{-3}$   
592 (min:  $0.2 \text{ ng m}^{-3}$  - max:  $1.8 \text{ ng m}^{-3}$ ). These levels are comparable to those measured in PM<sub>2.5</sub> by Mugica-Álvarez et al., (2016)  
593 in Veracruz (Mexico) but during the sugarcane non-harvest period. PM<sub>10</sub> BaP-MEQ levels in Araraquara (Brazil) (de Andrade  
594 et al., 2010; De Assuncao et al., 2014) were twice as high as those found in this study. This suggests that year-long sugarcane  
595 PHB in the CRV leads to lower mutagenic potentials compared to those at locations where the harvesting period (*zafra*) is  
596 shorter, thus with higher burning rates. We estimated the average BaP-TEQ and BaP-MEQ concentrations in the CRV  
597 according to their exposure to sugarcane burning products from Romero et al., (2013) data and used them as a benchmark to  
598 our measurements. PM<sub>10</sub>-bound BaP-TEQ and BaP-MEQ levels for areas not directly exposed to sugarcane burning were  $0.16$   
599  $\text{ng m}^{-3}$  and  $=0.21 \text{ ng m}^{-3}$ , respectively. Toxicity and mutagenicity due to PM<sub>10</sub>-bound PAHs were 4 times as high as those at  
600 areas directly exposed to sugarcane burning. It is reasonable to assume that PAHs are largely bound to fine aerosol ( $<2.5 \mu\text{m}$ ),  
601 thus that our measurements are comparable to (Romero et al., 2013). If so, our site at Palmira would be at an intermediate  
602 exposure condition, higher than areas not directly exposed to sugarcane burning but lower than directly exposed areas.

603  
604 Ratios among different PAHs have been extensively used to distinguish between traffic and other PAH sources. We used the  
605 diagnostic ratios presented by Ravindra et al. (2008) and Tobiszewski and Namieśnik (2012a) to better understand the  
606 contribution of sources to PM<sub>2.5</sub> in the CRV. The ratio benzo(e)pyrene to the sum of benzo(e)pyrene and benzo(a) pyrene is  
607 used as an indicator of aerosol aging. Local or “fresh” aerosols have  $[\text{BeP}]/([\text{BeP}]+[\text{BaP}])$  ratios around 0.5, while aged  
608 aerosols can have ratios as low as zero as a result of photochemical decomposition and oxidation. The  $[\text{BeP}]/([\text{BeP}]+[\text{BaP}])$   
609 ratio at Palmira was  $0.51 \pm 0.04$ , with a majority (84.4%,  $n = 38$ ) of fresh samples a minor fraction (15.6%,  $n=7$ ) of  
610 photochemically-degraded samples.

611  
612 Other two diagnostic ratios were used to assess the prevalence of traffic as a PM<sub>2.5</sub> source. The first ratio used IcdP/BghiP, two  
613 automobile emissions markers (Miguel and Pereira, 1989). Values higher than 0.5 for the ratio  $[\text{IcdP}]/([\text{IcdP}]+[\text{BghiP}])$   
614 indicates aged particles (Tobiszewski and Namieśnik, 2012) generated by coal, grass or wood burning (Yunker et al., 2002).  
615 The second ratio is  $[\text{BaP}]/[\text{BghiP}]$ . Ratios higher than 0.6 are indicative of traffic emissions (Tobiszewski and Namieśnik,  
616 2012). At Palmira, the  $[\text{IcdP}]/([\text{IcdP}]+[\text{BghiP}])$  and  $[\text{BaP}]/[\text{BghiP}]$  ratios were  $0.48 \pm 0.04$  and  $0.69 \pm 0.13$ , which indicates

617 that ~63% of the samples originated from combustion of oil products (n = 30), and ~36% came from non-traffic sources, like  
618 wood, grass, or coal (n = 15).

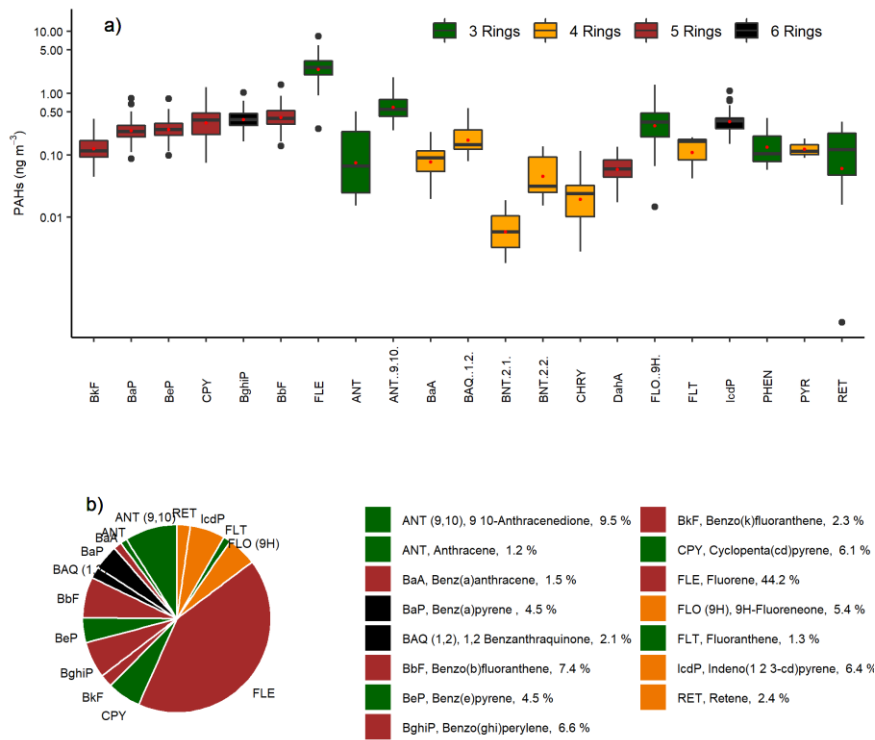
619

620 Also, the structure and size of PAHs are indicative of their sources. PAHs of low molecular weight (LMW) (two or three  
621 aromatic rings) have been reported as tracers of wood, grass, and fuel oil combustion, while those of medium molecular weight  
622 (MMW) (four rings) and high molecular height (HMW) (five and six rings) are associated with coal combustion and vehicular  
623 emissions. The ratio between LMW and the sum of MMW and HMW,  $LMW/(MMW+HMW)$ , is used for source identification.  
624 Ratios lower than one are indicative of oil products combustion, while ratios larger than one are associated with coal and  
625 biomass combustion (Tobiszewski and Namieśnik, 2012). The ratio at Palmira,  $LMW/(MMW+HMW) = 1.43 \pm 1.00$ , was  
626 rather variable but suggests that a large fraction of PAHs in CRV (82.2% of samples) were generated by biomass burning or  
627 combustion, as well as [coal combustion in brick kilns](#). Just one in five samples (17.8%) had PAHs attributable to oil product  
628 combustion.

629

630 Sugarcane-burning emitted PAH are mainly LMW, especially of two (~66% of PAHs) and three rings (~27%), among which  
 631 FLE, PHE and ANT are the most emitted, according to Hall et al. (2012) chemical profile. The relative abundance of three-

Con formato: Centrado



632 ring PAHs (

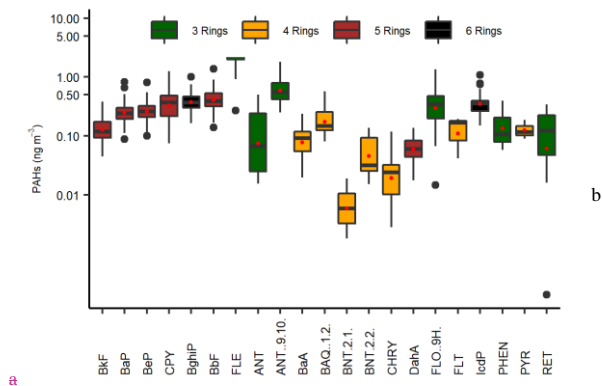
633 **Figure 4** in CRV's PM<sub>2.5</sub> is likely due to open-field sugarcane PHB to a major extent, and to controlled bagasse  
 634 combustion for electric power and steam production, to a lesser extent.

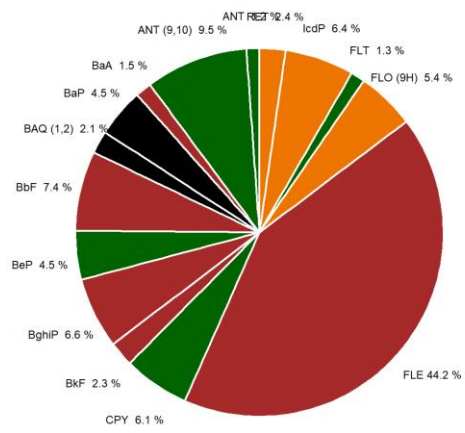
635

636 The highest PAH concentrations were observed on 10<sup>th</sup> August and 11<sup>th</sup> September 2018, with levels of 15.8 ng m<sup>-3</sup> and 14.4  
 637 ng m<sup>-3</sup>, respectively (Fig 5S). Elevated concentrations of 5 and 6 ring PAHs were observed on 10<sup>th</sup> August 2018. A change in  
 638 the wind circulation pattern was observed on the previous day (Fig S2), with a wind speed reduction and a predominance of

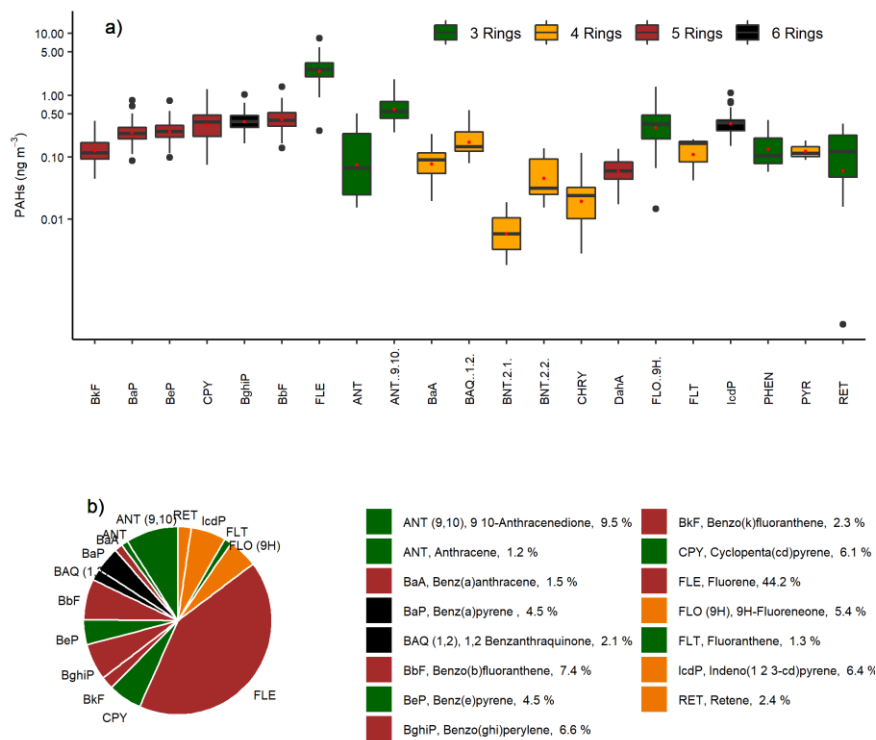
639 winds from the north. Later, on 11<sup>th</sup> September 2018, we observed an increase in 3-ring PAHs and winds from the NW at the  
 640 average wind speed at the sampling location. This indicates that there were at least two types of sources. The abundance of  
 641 HMW PAHs indicates fossil fuel combustion sources, and LMW PAHs suggest that parts of these come from non-fossil fuel  
 642 combustion sources.

643





b



Con formato: Centrado

644

645 Figure 4. The abundance of PAH<sub>s</sub> measured in PM<sub>2.5</sub> samples collected in CRV, represented by colors according to the number  
 646 of rings of each PAH, green (tree rings), yellow (four rings), brown (five rings), and black (six rings). a) Boxplot of  
 647 concentrations in ng m<sup>-3</sup>, red dots represent mean concentrations of each PAH. b) pie-plot of the relative abundance of PAH<sub>s</sub>  
 648 in PM<sub>2.5</sub> samples.

649 3.7. Alkanes

650

651 A total of 16 alkanes ranging from C<sub>20</sub> up to C<sub>34</sub> were analyzed in this study and used to identify the presence of fossil fuel  
652 combustion and plant fragments in the PM<sub>2.5</sub> samples. The abundance of total n-alkanes during the whole sampling period was  
653 in the range of 13.0 to 88.45 ng m<sup>-3</sup> with an average concentration of 40.36 ng m<sup>-3</sup> ± 18.82 ng m<sup>-3</sup>. In general, the high molecular  
654 weight n-alkanes such as C<sub>29</sub> – C<sub>31</sub> were the most abundant. These are characteristic of vegetative detritus corresponding to  
655 plant fragments in airborne PM (Lin et al., 2010). The most abundant n-alkanes were C<sub>29</sub>, C<sub>30</sub>, and C<sub>31</sub> (Fig 6.). Likewise, the  
656 carbon number maximum concentration (C<sub>max</sub>) was C<sub>29</sub> in 43% of samples and C<sub>31</sub> in 28% of them. This result is consistent  
657 with the chemical profile of sugarcane burning reported by (Oros et al., 2006) with a C<sub>max</sub> of C<sub>31</sub>.

658

659 The carbon preference index (CPI) and wax n-alkanes percentage (WNA%) are parameters used to elucidate the origin of the  
660 n-alkanes and infer whether emissions come from biogenic or anthropogenic sources. The CPI represents the ratio between  
661 odd and even carbon number n-alkanes. The equation used to calculate CPI in the present study is shown in [Table 2Table 2](#),  
662 following the procedure reported by (Marzi et al., 1993). Values of CPI ≤ 1 (or close to 1) indicate that n-alkanes are emitted  
663 from anthropogenic sources, while values higher than 1 indicate the influence of vegetative detritus and biomass burning in  
664 the PM<sub>2.5</sub> samples (Mancilla et al., 2016). In this study, the mean CPI was always greater than 1, with an average value of 1.22  
665 ± 0.18 (min:1.02 – max:1.8) that is between the CPI for fossil fuel emissions of ~1.0 (Caumo et al., 2020) and sugarcane  
666 burning of 2.1 (Oros et al., 2006), revealing the influence of several sources over the PM<sub>2.5</sub> in the CRV.

667

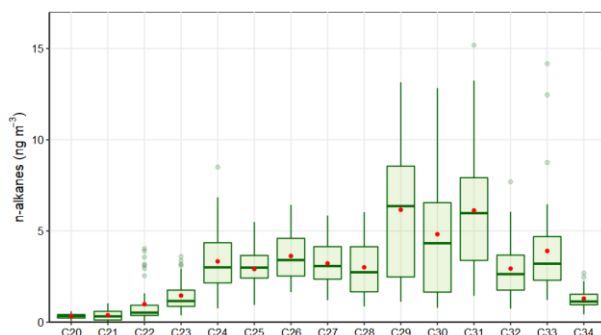
668 Likewise, WNA% represents the preference of odd n-alkanes in the sample. The odd n-alkanes, especially of higher molecular  
669 weight, are representative of plant wax related emissions. The waxes are present on the surface of plants, especially on the  
670 leaves, and they become airborne by a direct or indirect mechanism like wind action or biomass burning (Kang et al., 2018;  
671 Simoneit, 2002). In this research, the samples analyzed showed a preference for odd carbon on C<sub>27</sub>, C<sub>29</sub>, C<sub>31</sub> and C<sub>33</sub>, which  
672 have higher concentrations than the next higher and lower even carbon number homologs, proving the biogenic contribution  
673 over the PM<sub>2.5</sub> in the CRV. The WNA% was calculated using the equation shown in [Table 2Table 2](#), described by Yadav et  
674 al. (2013). A larger WNA% represents the contribution from emissions of plant waxes or biomass burning. Otherwise, a smaller  
675 value represents n-alkanes from petrogenic sources, known as petrogenic n-alkanes (PNA)%. The mean WNA% calculated  
676 for the PM<sub>2.5</sub> samples collected from the CRV was 12.65% ± 5.21% (min: 4.71% – max: 29.92%) and can be defined as  
677 petrogenic inputs (PNA%) that were 87.35% during the sampling period. The correlation between CPI and WNA was moderate  
678 (r<sup>2</sup>=0.53) supporting a consistent meaning between these two parameters, and they are useful for assessing the plant wax  
679 contribution to PM<sub>2.5</sub>.

680

681 Overall, the total concentration of n-alkanes in the PM<sub>2.5</sub> in the CRV was lower than those reported in areas where sugarcane  
682 is often burned in Brazil (Urban et al., 2016), although the behavior of the parameters of CPI and C<sub>max</sub> is similar. Compared  
683 with other urban areas in Latin America, the n-alkane concentration in the CRV was similar to that reported in the metropolitan

684 zone of the Mexican valley (MZMV) for  $PM_{2.5}$  (Amador-Muñoz et al., 2011), Bogota for  $PM_{10}$  and slightly lower than reported  
 685 in Sao Paulo for  $PM_{10}$  (Vasconcellos et al., 2011). However, the CPI and WNA in these cities were smaller than in the CRV,  
 686 because of the strong influence of vehicular emissions in these densely populated cities. The OC/EC ratio was moderately  
 687 associated with WNA values ( $r^2 = 0.41$ ), indicating that an increase in this ratio can be explained by the vegetative detritus  
 688 contribution to  $PM_{2.5}$ , while the levoglucosan concentrations did not show correspondence to the CPI and WNA values;  
 689 therefore, the levoglucosan levels did not explain the preference of odd carbon number homologs. These results indicated that  
 690 the n-alkanes found in this study came from several sources, with a noticeable contribution from plant wax emissions. The  
 691 parameters used to assess the source contribution of  $PM_{2.5}$  through n-alkanes such as CPI and WNA%, were characteristic of  
 692 aerosols collected in urban areas.

693



694

695

Figure 5. Average n-alkanes concentrations in  $PM_{2.5}$  samples

### 696 3.8. $PM_{2.5}$ mass closure

697

698 Mass closure (Figure 6) shows the crucial contribution of organic material ( $52.66 \pm 18.44\%$ ) and inorganic fraction,  
 699 represented by sulfate ( $12.69 \pm 2.84\%$ ), ammonium ( $3.75 \pm 1.05\%$ ), nitrate ( $2.56 \pm 1.29\%$ ). EC constituted  $7.13 \pm 2.44\%$  of  
 700  $PM_{2.5}$ . The mineral fraction corresponded to dust ( $3.51 \pm 1.35\%$ ) and TEO ( $0.85 \pm 0.42\%$ ). Mass closure of  $88.42 \pm 24.17\%$   
 701 was achieved. Although  $PM_{2.5}$  concentrations observed in the CRV were not so high as compared with those registered in  
 702 Brazil and Mexico during the preharvest season, the EC percentage is in a similar range or slightly lower than those observed  
 703 in other urban areas (Snider et al., 2016), showing the key role of incomplete combustion processes in the area.

704

705 The average (OC/EC) ratio found in CRV was  $4.2 \pm 0.72$ , from which we can infer that secondary aerosol formation had a  
 706 relevant role. The segregation of OC into the primary and secondary fractions was carried out using two methods. The first



707 was the EC tracer method applied in previous studies (Pio et al., 2011; Plaza et al., 2011), and the second was the organic  
708 tracer method, which is based on the lineal regression between OC and organic tracers from primary sources. In the EC tracer  
709 method, the  $(OC/EC)_{\min}$  ratio selected to differentiate  $OC_{\text{prim}}$  from  $OC_{\text{sec}}$  was the minimum ratio observed, equivalent to 2.12.  
710 Still, this value could induce the overestimation of  $OC_{\text{prim}}$  due to the distance between the emission sources and the sampling  
711 site (27 m aboveground), and the local meteorological conditions that favor the volatilization and oxidation of organic  
712 components into particles before being collected. As a result,  $OC_{\text{prim}}$  was estimated at 50.3% and  $OC_{\text{sec}}$  at 49.7% of the total  
713 OC, with a minimum variability of 3.8%. The estimated  $OM_{\text{pri}}$  concentration was  $3.22 \pm 1.09 \mu\text{g m}^{-3}$  and the  $OM_{\text{sec}}$   
714 concentration was  $4.01 \pm 1.78 \mu\text{g m}^{-3}$ , which represented 24.2% and 28.5% of  $PM_{2.5}$  respectively.

715

716 In the organic tracer method, the contribution of fossil fuel combustion - mainly derived from transport -, biomass burning,  
717 and vegetative detritus to  $OC_{\text{prim}}$  was estimated from a [linear model by robust regression using an M estimator with bisquare](#)  
718 [function linear relationship](#) between organic tracers and OC. Resulting contributions were as follows:  $OC_{\text{ff}}$ : 16.38%,  $OC_{\text{bb}}$ :  
719 15.19%, and  $OC_{\text{det}}$ : 1.45% of total OC measured. Overall, the use organic tracer method to estimate  $OC_{\text{prim}}$  indicates that this  
720 carbonaceous fraction represents  $32.68\% \pm 11.02\%$  of total OC, and it may fluctuate between 17.61% and 68.60%.

721

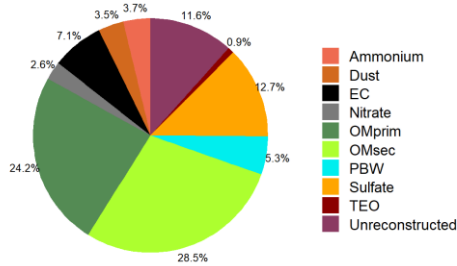
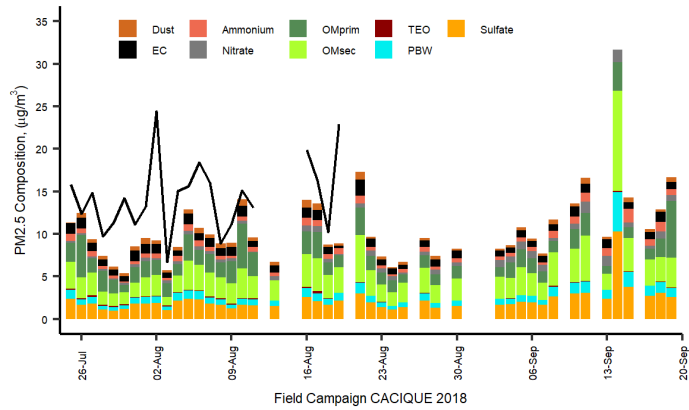
722 The difference between  $OC_{\text{prim}}$  from the organic tracer method and that obtained from the EC tracer method can be associated  
723 to the fact that the organic tracer method may not be representative of all sources. Industrial coal and fuel oil burning, garbage  
724 burning, cooking, charcoal production and other sources may not be accounted for by this method, since we did not have  
725 specific organic tracers for each of these activities.

726

727 The mineral fraction, quantified as the sum of the oxides present in the crustal material (dust) and other TEO contributed  $3.51 \pm$   
728  $1.35\%$  and  $0.85 \pm 0.42\%$ , respectively. Despite the non-quantification of highly abundant mineral dust elements such as Si,  
729 the concentrations of Ca, Ti, and Fe indicated the impact of soil resuspension on the  $PM_{2.5}$  mass concentration.

730

731 PBW depends on the concentration of hygroscopic compounds embodied in the PM and the relative humidity of the weighing  
732 room where  $PM_{2.5}$  mass collected on the filters was determined. In this study, it was assumed that (i)  $NH_4^+$ ,  $SO_4^{2-}$  and  $NO_3^-$   
733 were the main compounds responsible for absorbed water and (ii) thermodynamic equilibrium is dominated by these ions that  
734 allow calculating the  $H^+$  molar fraction as a difference between  $(SO_4^{2-} + NO_3^-)$  and  $NH_4^+$ , which is required to establish charge  
735 neutrality. Polar organic compounds and other water-soluble ions were not considered in the present study. The PBW content  
736 was estimated using the mean measured concentrations of  $NH_4^+$ ,  $SO_4^{2-}$  and  $NO_3^-$  in the AIM Model, where a multiplier factor  
737 of 0.32 was found as a proportion between the concentrations of the sum of these ions and the water fraction contained in  
738  $PM_{2.5}$ . As a result, PBW was 5.3% of the  $PM_{2.5}$  mass concentration.



739

740

741

742

743

744

745

Figure 6. Mass reconstruction of PM<sub>2.5</sub> collected in CRV. Figure in upper corresponding to timeseries of PM<sub>2.5</sub> gravimetric mass measured and reconstructed mass from the chemical speciation in CRV during July – September 2018 and lower is the pie plot the relative mean contributions (%) of major chemical components of gravimetric PM<sub>2.5</sub> based on chemical speciation.

#### 746 4. Conclusions

747 PM<sub>2.5</sub> samples collected in the Cauca River Valley, Colombia, were analyzed to determine the main chemical components of  
748 fine aerosol particles and to qualitatively identify aerosol sources using its chemical composition and diagnostic ratios. PM<sub>2.5</sub>  
749 during the campaign was  $14.4 \pm 4.4 \mu\text{g m}^{-3}$ . Its main components were OC ( $4.0 \pm 1.3 \mu\text{g m}^{-3}$ ), sulfate ( $2.2 \pm 1.4 \mu\text{g m}^{-3}$ ), and  
750 EC ( $1.0 \pm 0.3 \mu\text{g m}^{-3}$ ), ammonium ( $0.7 \pm 0.6 \mu\text{g m}^{-3}$ ), and nitrate ( $0.5 \pm 0.3 \mu\text{g m}^{-3}$ ). OM was estimated using the EC tracer  
751 method and the organic tracer method. Mass closure using the EC tracer method explained 88.4% of PM<sub>2.5</sub>, whereas the organic  
752 tracer method explained 70.9% of PM<sub>2.5</sub>. We attribute this difference to the lack of information of specific organic tracers for  
753 some sources, both primary and secondary. Organic material and inorganic ions were the dominant groups of species,  
754 constituting almost 79% of PM<sub>2.5</sub>. OM<sub>prim</sub> and OM<sub>sec</sub> from the EC tracer method contribute 24.2% and 28.5% to PM<sub>2.5</sub>.  
755 Inorganic ions made up 19.0%, EC 7.1%, dust 3.5%, PBW 5.3%, and TEO 0.9% of PM<sub>2.5</sub>.

756  
757 Aerosol acidity was evaluated using three methods. The first, using the nitrate/sulfate ratio; the second using the anion/cation  
758 equivalent ratio; and the third, estimating the pH with the E-AIM thermodynamic model. All methods showed that the aerosol  
759 was acidic, with a pH of  $2.5 \pm 0.4$ , mainly because of the abundance of organic and sulfur compounds.

760  
761 Diagnostic ratios applied to organic compounds indicate that most PM<sub>2.5</sub> was emitted locally and had contributions of both  
762 pyrogenic and petrogenic sources. In addition, levoglucosan and mannosan levels showed that biomass burning was ubiquitous  
763 during the sampling period. Fluoranthene (FLE) was the most abundant PAH, confirming the strong influence of BB associated  
764 with agro-industry. Five- and six-ring PAH associated with vehicular emissions were also abundant in PM<sub>2.5</sub>. Our  
765 measurements point to BB as the main source of PAHs in CRV. Relatively low PM<sub>2.5</sub> concentrations and mutagenic potentials  
766 are consistent with low-intensity, year-long BB and sugarcane PHB in CRV, which leads to lower atmospheric pollutant  
767 burdens and mutagenic potentials compared to those at locations where the harvesting period is shorter (*zafra*) thus with higher  
768 burning rates.

769 *Author contribution:* RJ, GR-S, and NR conceived and managed the project. LM-F, ACV-B, GR-S, and RJ set the instruments  
770 up and performed the aerosol sampling. LM-F carried out the sample chemical analysis at TROPOS with the guidance and  
771 support of DvP, MvP, KW, and HH. LM-F and ACV-B analyzed the measurement results, including PCA and other techniques  
772 with the support of DvP and LM-F, RJ, NR and ACV-B prepared the manuscript with substantial contributions from all the  
773 authors.

774 *Competing interests:* The authors declare that they have no conflict of interest.

775 *Acknowledgments:* The authors gratefully acknowledge the financial support from Universidad Nacional de Colombia – Sede  
 776 Palmira (Project “Impacto de la quema de caña de azúcar en la calidad del aire del Valle Geografico del Río Cauca  
 777 (CACIQUE), –Hermes # 37718), and Leibniz Institute for Tropospheric Research (TROPOS) for analytical support. This  
 778 project was supported by EU granted the mobility project PAPILA. We thank Susanne Fuchs, Anke Roedger, Sylvia  
 779 Haferkorn, and Kornelia Pielok for their technical assistance in the chemical analysis of samples. We acknowledge Pablo  
 780 Gutierrez for his contributions in the processing of the open sugarcane burning database and for preparing the CRV map.

## 781 **References**

- 782 Aerocivil: Estadísticas Operacionales, Operaciones aéreas Total. 2000-2019  
 783 <https://www.aerocivil.gov.co/atencion/estadisticas-de-las-actividades-aeronauticas/estadisticas-operacionales>, last access: 15  
 784 February 2022, 2019.
- 785 Agarwal, A., Satsangi, A., Lakhani, A. and Kumari, K. M.: Seasonal and spatial variability of secondary inorganic aerosols in  
 786 PM<sub>2.5</sub> at Agra: Source apportionment through receptor models, *Chemosphere*, 242, 125132,  
 787 <https://doi.org/10.1016/j.chemosphere.2019.125132>, 2020.
- 788 Alvi, M. U., Kistler, M., Shahid, I., Alam, K., Chishtie, F., Mahmud, T. and Kasper-Giebl, A.: Composition and source  
 789 apportionment of saccharides in aerosol particles from an agro-industrial zone in the Indo-Gangetic Plain, *Environ. Sci. Pollut.*  
 790 *Res.* 2020 2712, 27(12), 14124–14137, <https://doi.org/10.1007/S11356-020-07905-2>, 2020.
- 791 Amador-Muñoz, O., Villalobos-Pietrini, R., Miranda, J. and Vera-Avila, L. E.: Organic compounds of PM<sub>2.5</sub> in Mexico  
 792 Valley: Spatial and temporal patterns, behavior and sources, *Sci. Total Environ.*, 409(8), 1453–1465,  
 793 <https://doi.org/10.1016/j.scitotenv.2010.11.026>, 2011.
- 794 de Andrade, S. J., Cristale, J., Silva, F. S., Julião Zocolo, G. and Marchi, M. R. R.: Contribution of sugar-cane harvesting  
 795 season to atmospheric contamination by polycyclic aromatic hydrocarbons (PAHs) in Araraquara city, Southeast Brazil,  
 796 *Atmos. Environ.*, 44(24), 2913–2919, <https://doi.org/10.1016/j.atmosenv.2010.04.026>, 2010.
- 797 Andreae, M. O.: Soot Carbon and Excess Fine Potassium : Long-Range Transport of Combustion-Derived Aerosols., 1983.
- 798 Aneja, V. P., Schlesinger, W. H. and Erisman, J. W.: Farming pollution, *Nat. Geosci.*, 1(7), 409–411,  
 799 <https://doi.org/10.1038/ngeo236>, 2008.
- 800 Aneja, V. P., Schlesinger, W. H. and Erisman, J. W.: Effects of agriculture upon the air quality and climate: Research, policy,  
 801 and regulations, *Environ. Sci. Technol.*, 43(12), 4234–4240, <https://doi.org/10.1021/es8024403>, 2009.
- 802 Asocaña: Aspectos Generales del Sector Agroindustrial de la Caña 2017 - 2018. Informe Anual. <https://www.asocana.org>,  
 803 2018.
- 804 Asocaña: Aspectos generales del sector agroindustrial de la caña Informe anual 2018-2019.  
 805 [https://www.asocana.org/documentos/2352019-D0CA1EED-  
 806 00FF00,000A0000,878787,C3C3C3,0F0F0F,B4B4B4,FF00FF,2D2D2D,A3C4B5.pdf](https://www.asocana.org/documentos/2352019-D0CA1EED-00FF00,000A0000,878787,C3C3C3,0F0F0F,B4B4B4,FF00FF,2D2D2D,A3C4B5.pdf), last access: 20 May 2020, 2019.

Con formato: Español (Colombia)

Con formato: Español (Colombia)

Código de campo cambiado

Con formato: Español (Colombia)

- 807 De Assuncao, J. V., Pesquero, C. R., Nardocci, A. C., Francisco, A. P., Soares, N. S. and Ribeiro, H.: Airborne polycyclic  
 808 aromatic hydrocarbons in a medium-sized city affected by preharvest sugarcane burning and inhalation risk for human health,  
 809 *J. Air Waste Manag. Assoc.*, 64(10), 1130–1139, <https://doi.org/10.1080/10962247.2014.928242>, 2014.
- 810 Begam, G. R., Vachaspati, C. V., Ahammed, Y. N., Kumar, K. R., Reddy, R. R., Sharma, S. K., Saxena, M. and Mandal, T.  
 811 K.: Seasonal characteristics of water-soluble inorganic ions and carbonaceous aerosols in total suspended particulate matter at  
 812 a rural semi-arid site, Kadapa (India), *Environ. Sci. Pollut. Res.*, 24(2), 1719–1734, [https://doi.org/10.1007/s11356-016-7917-](https://doi.org/10.1007/s11356-016-7917-1)  
 813 1, 2016.
- 814 Bhattarai, H., Saikawa, E., Wan, X., Zhu, H., Ram, K., Gao, S., Kang, S., Zhang, Q., Zhang, Y., Wu, G., Wang, X., Kawamura,  
 815 K., Fu, P. and Cong, Z.: Levoglucosan as a tracer of biomass burning: Recent progress and perspectives, *Atmos. Res.*,  
 816 220(November 2018), 20–33, <https://doi.org/10.1016/j.atmosres.2019.01.004>, 2019.
- 817 Boman, J., Lindén, J., Thorsson, S., Holmer, B. and Eliasson, I.: A tentative study of urban and suburban fine particles (PM<sub>2.5</sub>)  
 818 collected in Ouagadougou, Burkina Faso, *X-Ray Spectrom.*, 38(4), 354–362, <https://doi.org/10.1002/XRS.1173>, 2009.
- 819 Cardozo-Valencia, A., Saa, G. R., Hernandez, A. J., Lopez, G. R. and Jimenez, R.: Distribución espaciotemporal y estimación  
 820 de emisiones por quema precosecha de caña de azúcar en el Valle del Cauca, *Conf. Proc. - Congr. Colomb. y Conf. Int. Calid.*  
 821 *Aire y Salud Publica, CASAP 2019*, <https://doi.org/10.1109/CASAP.2019.8916696>, 2019.
- 822 Casey, K. D., Bicudo, J. R., Schmidt, D. R., Singh, A., Gay, S. W., Gates, R. S., Jacobson, L. D. and Hoff, S. J.: Air quality  
 823 and emissions from livestock and poultry production / waste management systems, in *Animal Agriculture and the*  
 824 *Environment, National Center for Manure & Animal Waste Management White Papers*, pp. 1–40, , 2006.
- 825 Caumo, S., Bruns, R. E. and Vasconcellos, P. C.: Variation of the distribution of atmospheric n-alkanes emitted by different  
 826 fuels' combustion, *Atmosphere (Basel)*, 11(6), 1–19, <https://doi.org/10.3390/atmos11060643>, 2020.
- 827 Cavalli, F., Viana, M., Yttri, K. E., Genberg, J. and Putaud, J.: Toward a standardised thermal-optical protocol for measuring  
 828 atmospheric organic and elemental carbon: the EUSAAR protocol, *Atmos. Meas. Tech.*, 3, 79–89,  
 829 <https://doi.org/10.5194/amt-3-79-2010>, 2010.
- 830 Chow, J. C., Lowenthal, D. H., Chen, L. W. A., Wang, X. and Watson, J. G.: Mass reconstruction methods for PM<sub>2.5</sub>: a  
 831 review, *Air Qual. Atmos. Heal.*, 8(3), 243–263, <https://doi.org/10.1007/s11869-015-0338-3>, 2015.
- 832 Clegg, S. L., Brimblecombe, P. and Wexler, A. S.: Thermodynamic Model of the System H<sup>+</sup>–NH<sub>4</sub><sup>+</sup>–SO<sub>4</sub><sup>2-</sup>–NO<sub>3</sub>–H<sub>2</sub>O at  
 833 Tropospheric Temperatures, *J. Phys. Chem. A*, 102(12), 2137–2154, <https://doi.org/10.1021/jp973042r>, 1998.
- 834 Criollo, J. and Daza, N.: Evaluación de los niveles de concentración de metales en PM 10 producto de la quema de biomasa  
 835 en el valle geográfico del río Cauca, La Salle University [https://ciencia.lasalle.edu.co/ing\\_ambiental\\_sanitaria/135%0AThis](https://ciencia.lasalle.edu.co/ing_ambiental_sanitaria/135%0AThis),  
 836 2011.
- 837 Dabek-Zlotorzynska, E., Dann, T. F., Kalyani Martinelango, P., Celso, V., Brook, J. R., Mathieu, D., Ding, L. and Austin, C.  
 838 C.: Canadian National Air Pollution Surveillance (NAPS) PM<sub>2.5</sub> speciation program: Methodology and PM<sub>2.5</sub> chemical  
 839 composition for the years 2003–2008, *Atmos. Environ.*, 45(3), 673–686, <https://doi.org/10.1016/j.atmosenv.2010.10.024>,

Con formato: Español (Colombia)

Con formato: Español (Colombia)

- 840 2011.
- 841 Durant, J. L., Busby Jr, W. F., Lafleur, A. L., Penman, B. W. and Crespi, C. L.: Human cell mutagenicity of oxygenated,  
842 nitrated and unsubstituted polycyclic aromatic hydrocarbons associated with urban aerosols, *Mutat. Res. - Genet. Toxicol.*,  
843 371(3–4), 123–157, [https://doi.org/10.1016/S0165-1218\(96\)90103-2](https://doi.org/10.1016/S0165-1218(96)90103-2), 1996.
- 844 El-Zanan, H. S., Lowenthal, D. H., Zielinska, B., Chow, J. C. and Kumar, N.: Determination of the organic aerosol mass to  
845 organic carbon ratio in IMPROVE samples, *Chemosphere*, 60(4), 485–496,  
846 <https://doi.org/10.1016/j.chemosphere.2005.01.005>, 2005.
- 847 Engling, G., Lee, J. J., Tsai, Y.-W., Lung, S.-C. C., Chou, C. C.-K. and Chan, C.-Y.: Size-Resolved Anhydrosugar Composition  
848 in Smoke Aerosol from Controlled Field Burning of Rice Straw, *Aerosol Sci. Technol.*, 43(7), 662–672,  
849 <https://doi.org/10.1080/02786820902825113>, 2009.
- 850 FAO: FAOSTAT, <http://www.fao.org/faostat/en/#data/QC>, last access: 21 July 2021a, 2020.
- 851 FAO: FAOSTAT, <http://www.fao.org/faostat/en/#data/QC>, 2020b.
- 852 Fomba, K. ., Müller, K., Van Pinxteren, D. and Herrmann, H.: Aerosol size-resolved trace metal composition in remote  
853 northern tropical Atlantic marine environment: case study Cape Verde islands, *Atmos. Chem. Phys.*, 13(9), 4801–4814,  
854 <https://doi.org/10.5194/acp-13-4801-2013>, 2013.
- 855 Fomba, K. W., van Pinxteren, D., Müller, K., Spindler, G. and Herrmann, H.: Assessment of trace metal levels in size-resolved  
856 particulate matter in the area of Leipzig, *Atmos. Environ.*, 176, <https://doi.org/10.1016/j.atmosenv.2017.12.024>, 2018.
- 857 Franzin, B. T., Guizzellini, F. C., de Babos, D. V., Hojo, O., Pastre, I. A., Marchi, M. R. R., Fertonani, F. L. and Oliveira, C.  
858 M. R. R.: Characterization of atmospheric aerosol (PM10 and PM2.5) from a medium sized city in São Paulo state, Brazil, *J.*  
859 *Environ. Sci. (China)*, 89, 238–251, <https://doi.org/10.1016/j.jes.2019.09.014>, 2020.
- 860 Friese, E. and Ebel, A.: Temperature Dependent Thermodynamic Model of the System  $H + - NH_4 + - Na + - SO_4 - - NO_3$   
861  $- - Cl - - H_2O$ , 2010.
- 862 Gonçalves, C., Figueiredo, B. R., Alves, C. A., Cardoso, A. A. and Vicente, A. M.: Size-segregated aerosol chemical  
863 composition from an agro-industrial region of São Paulo state, Brazil, *Air Qual. Atmos. Heal.* 2016 104, 10(4), 483–496,  
864 <https://doi.org/10.1007/S11869-016-0441-0>, 2016.
- 865 Gondwe, M.: Comparison of modeled versus measured MSA : nss  $SO_4$  ratios : A global analysis, , 18, 1–18,  
866 <https://doi.org/10.1029/2003GB002144>, 2004.
- 867 H M Malcolm and Dobson, S.: The calculation of an Environmental Assessment Level (EAL) for atmospheric PAHs using  
868 relative potencies., 1994.
- 869 Hall, D., Wu, C. Y., Hsu, Y. M., Stormer, J., Engling, G., Capeto, K., Wang, J., Brown, S., Li, H. W. and Yu, K. M.: PAHs,  
870 carbonyls, VOCs and PM 2.5 emission factors for pre-harvest burning of Florida sugarcane, *Atmos. Environ.*, 55, 164–172,  
871 <https://doi.org/10.1016/j.atmosenv.2012.03.034>, 2012.
- 872 Hernández, J. D. R. and Mesa, Ó. J.: A simple conceptual model for the heat induced circulation over Northern South America

- 873 and MESO-America, *Atmosphere (Basel)*, 11(11), 1–14, <https://doi.org/10.3390/atmos11111235>, 2020.
- 874 Ianniello, A., Spataro, F., Esposito, G., Allegrini, I., Hu, M. and Zhu, T.: and Physics Chemical characteristics of inorganic  
875 ammonium salts in PM<sub>2.5</sub> in the atmosphere of Beijing ( China ) , (October), <https://doi.org/10.5194/acp-11-10803-2011>,  
876 2011.
- 877 Iinuma, Y., Engling, G., Puxbaum, H. and Herrmann, H.: A highly resolved anion-exchange chromatographic method for  
878 determination of saccharidic tracers for biomass combustion and primary bio-particles in atmospheric aerosol, *Atmos.*  
879 *Environ.*, 43(6), 1367–1371, 2009.
- 880 Jorquera, H. and Barraza, F.: Source apportionment of ambient PM<sub>2.5</sub> in Santiago, Chile: 1999 and 2004 results, *Sci. Total*  
881 *Environ.*, 435–436, 418–429, <https://doi.org/10.1016/j.scitotenv.2012.07.049>, 2012.
- 882 Jorquera, H. and Barraza, F.: Source apportionment of PM<sub>10</sub> and PM<sub>2.5</sub> in a desert region in northern Chile, *Sci. Total*  
883 *Environ.*, 444, 327–335, <https://doi.org/10.1016/j.scitotenv.2012.12.007>, 2013.
- 884 Kang, M., Ren, L., Ren, H., Zhao, Y., Kawamura, K., Zhang, H., Wei, L., Sun, Y., Wang, Z. and Fu, P.: Primary biogenic and  
885 anthropogenic sources of organic aerosols in Beijing, China: Insights from saccharides and n-alkanes, *Environ. Pollut.*, 243,  
886 1579–1587, <https://doi.org/10.1016/j.envpol.2018.09.118>, 2018.
- 887 Karagulian, F., Belis, C. A., Francisco, C., Dora, C., Prüss-üstün, A. M., Bonjour, S., Adair-rohani, H. and Amann, M.:  
888 Contributions to cities ' ambient particulate matter ( PM ): A systematic review of local source contributions at global level,  
889 *Atmos. Environ.*, 120, 475–483, <https://doi.org/10.1016/j.atmosenv.2015.08.087>, 2015.
- 890 Khedidji, S., Müller, K., Rabhi, L., Spindler, G., Fomba, K. W., Pinxteren, D. van, Yassaa, N. and Herrmann, H.: Chemical  
891 Characterization of Marine Aerosols in a South Mediterranean Coastal Area Located in Bou Ismaïl, Algeria, *Aerosol Air Qual.*  
892 *Res.*, 20(January), <https://doi.org/10.4209/aaqr.2019.09.0458>, 2020.
- 893 Kundu, S. and Stone, E. A.: Composition and sources of fine particulate matter across urban and rural sites in the Midwestern  
894 United States, *Environ. Sci. Process. Impacts*, 16(6), 1360–1370, <https://doi.org/10.1039/c3em00719g>, 2014.
- 895 Lara, L. L., Artaxo, P., Martinelli, L. A., Camargo, P. B., Victoria, R. L. and Ferraz, E. S. B.: Properties of aerosols from  
896 sugar-cane burning emissions in Southeastern Brazil, *Atmos. Environ.*, 39(26), 4627–4637,  
897 <https://doi.org/10.1016/j.atmosenv.2005.04.026>, 2005.
- 898 Lee, S., Wang, Y. and Russell, A. G.: Assessment of secondary organic carbon in the southeastern United States: A review, *J.*  
899 *Air Waste Manag. Assoc.*, 60(11), 1282–1292, <https://doi.org/10.3155/1047-3289.60.11.1282>, 2010.
- 900 Lee, T., Yu, X., Kreidenweis, S. M., Malm, W. C. and Collett, J. L.: Semi-continuous measurement of PM<sub>2.5</sub> ionic  
901 composition at several rural locations in the United States, , 42, 6655–6669, <https://doi.org/10.1016/j.atmosenv.2008.04.023>,  
902 2008.
- 903 Li, J., Song, Y., Mao, Y., Mao, Z., Wu, Y., Li, M., Huang, X., He, Q. and Hu, M.: Chemical characteristics and source  
904 apportionment of PM<sub>2.5</sub> during the harvest season in eastern China's agricultural regions, *Atmos. Environ.*, 92, 442–448,  
905 <https://doi.org/10.1016/J.ATMOSENV.2014.04.058>, 2014.

- 906 Li, X., Wang, L., Ji, D., Wen, T., Pan, Y., Sun, Y. and Wang, Y.: Characterization of the size-segregated water-soluble  
 907 inorganic ions in the Jing-Jin-Ji urban agglomeration: Spatial/temporal variability, size distribution and sources, *Atmos.*  
 908 *Environ.*, 77, 250–259, <https://doi.org/10.1016/j.atmosenv.2013.03.042>, 2013.
- 909 Liang, C. S., Duan, F. K., He, K. Bin and Ma, Y. L.: Review on recent progress in observations, source identifications and  
 910 countermeasures of PM<sub>2.5</sub>, *Environ. Int.*, 86, 150–170, <https://doi.org/10.1016/j.envint.2015.10.016>, 2016.
- 911 Lin, L., Lee, M. L. and Eatough, D. J.: Review of recent advances in detection of organic markers in fine particulate matter  
 912 and their use for source apportionment, *J. Air Waste Manag. Assoc.*, 60(1), 3–25, <https://doi.org/10.3155/1047-3289.60.1.3>,  
 913 2010.
- 914 López Larada, J.: |Zona portuaria de Buenaventura: y su importancia en Colombia, Univ. San Buenaventura, 1–14  
 915 [http://bibliotecadigital.usbcali.edu.co/bitstream/10819/7099/1/Zona\\_Portuaria\\_Buenaventura\\_Lopez\\_2017.pdf](http://bibliotecadigital.usbcali.edu.co/bitstream/10819/7099/1/Zona_Portuaria_Buenaventura_Lopez_2017.pdf), last access:  
 916 23 February 2022, 2017.
- 917 Lopez, M. and Howell, W.: Katabatic Winds in the equatorial Andes, *J. Atmos. Sci.*, 24(1), 29–35, 1967.
- 918 Lyu, R., Shi, Z., Alam, M. S., Wu, X., Liu, D., Vu, T. V., Stark, C., Xu, R., Fu, P., Feng, Y. and Harrison, R. M.: Alkanes and  
 919 aliphatic carbonyl compounds in wintertime PM<sub>2.5</sub> in Beijing, China, *Atmos. Environ.*, 202(November 2018), 244–255,  
 920 <https://doi.org/10.1016/j.atmosenv.2019.01.023>, 2019.
- 921 MADS: Res. No 2254, Ministerio de Ambiente y Desarrollo Sostenible, Colombia., 2017.
- 922 Majra, J. P.: Air Quality in Rural Areas, in *Chemistry, Emission Control, Radioactive Pollution and Indoor Air Quality*,  
 923 <https://doi.org/10.5772/16890>, , 2011.
- 924 Mancilla, Y., Mendoza, A., Fraser, M. P. and Herckes, P.: Organic composition and source apportionment of fine aerosol at  
 925 Monterrey, Mexico, based on organic markers, *Atmos. Chem. Phys.*, 16(2), 953–970, [https://doi.org/10.5194/acp-16-953-](https://doi.org/10.5194/acp-16-953-2016)  
 926 2016, 2016.
- 927 Marzi, R., Torkelson, B. E. and Olson, R. K.: A revised carbon preference index, *Org. Geochem.*, 20(8), 1303–1306,  
 928 [https://doi.org/10.1016/0146-6380\(93\)90016-5](https://doi.org/10.1016/0146-6380(93)90016-5), 1993.
- 929 Meinardi, S., Simpson, I. J., Blake, N. J., Blake, D. R. and Rowland, F. S.: Dimethyl disulfide (DMDS) and dimethyl sulfide  
 930 (DMS) emissions from biomass burning in Australia, *Geophys. Res. Lett.*, 30(9), <https://doi.org/10.1029/2003GL016967>,  
 931 2003.
- 932 Mesa S., Ó. J. and Rojo H., J. D.: On the general circulation of the atmosphere around Colombia, *Rev. la Acad. Colomb.*  
 933 *Ciencias Exactas, Fis. y Nat.*, 44(172), 857–875, <https://doi.org/10.18257/RACCEFYN.899>, 2020.
- 934 Miguel, A. H. and Pereira, P. A. P.: Benzo(k)fluoranthene, benzo(ghi)perylene, and indeno(1, 2, 3-cd)pyrene: New tracers of  
 935 automotive emissions in receptor modeling, *Aerosol Sci. Technol.*, 10(2), 292–295,  
 936 <https://doi.org/10.1080/02786828908959265>, 1989.
- 937 Min.Agricultura: Cadenas cárnicas bovina - bufalina, Bogotá D.C.  
 938 <https://sioc.minagricultura.gov.co/Bovina/Documentos/2018-12-30 Cifras Sectoriales.pdf>, 2018.

Con formato: Español (Colombia)

Con formato: Español (Colombia)

Con formato: Español (Colombia)

Con formato: Español (Colombia)



- 939 Min.Agricultura: Cadena Carnica Porcina, Bogotá D.C. <https://sioc.minagricultura.gov.co/Porcina/Documentos/2019-12-30>  
 940 Cifras sectoriales.pdf, 2019.
- 941 Min.Agricultura: Cadena Avícola, segundo trimestre 2020, Bogotá D.C.  
 942 <https://www.minagricultura.gov.co/paginas/default.aspx>, 2020.
- 943 [Mugica-Álvarez, V., Santiago-de la Rosa, N., Figueroa-Lara, J., Flores-Rodríguez, J., Torres-Rodríguez, M. and Magaña-Reyes, M.:](#) Emissions of PAHs derived from sugarcane burning and processing in Chiapas and Morelos México, *Sci. Total Environ.*, 527–528, 474–482, <https://doi.org/10.1016/j.scitotenv.2015.04.089>, 2015.
- 944 [Mugica-Álvarez, V., Ramos-Guizar, S., Rosa, N. S. la, Torres-Rodríguez, M. and Noreña-Franco, L.:](#) Black Carbon and Particulate Organic Toxics Emitted by Sugarcane Burning in Veracruz, México, *Int. J. Environ. Sci. Dev.*, 7(4), 290–294, <https://doi.org/10.7763/ijesd.2016.v7.786>, 2016.
- 945 [Mugica-Álvarez, V., Hernández-Rosas, F., Magaña-Reyes, M., Herrera-Murillo, J., Santiago-De La Rosa, N., Gutiérrez-Arzaluz, M., de Jesús Figueroa-Lara, J. and González-Cardoso, G.:](#) Sugarcane burning emissions: Characterization and emission factors, *Atmos. Environ.*, 193, 262–272, <https://doi.org/10.1016/j.atmosenv.2018.09.013>, 2018.
- 946 [Murillo, J. H., Roman, S. R., Felix, J., Marin, R., Ramos, A. C., Jimenez, S. B., Gonzalez, B. C. and Baumgardner, D. G.:](#) Chemical characterization and source apportionment of PM10 and PM2.5 in the metropolitan area of Costa Rica, *Central America Jorge, Atmos. Pollut. Res.*, 4(2), 181–190, <https://doi.org/10.5094/APR.2013.018>, 2013.
- 947 [Neuß, C., Pelzing, M., Plewka, A. and Herrmann, H.:](#) A new analytical approach for size-resolved speciation of organic compounds in atmospheric aerosol particles: Methods and first results, *J. Geophys. Res. Atmos.*, 105(D4), 4513–4527, <https://doi.org/10.1029/1999JD901038>, 2000.
- 948 [Nisbet, I. C. T. and LaGoy, P. K.:](#) Toxic equivalency factors (TEFs) for polycyclic aromatic hydrocarbons (PAHs), *Regul. Toxicol. Pharmacol.*, 16(3), 290–300, [https://doi.org/10.1016/0273-2300\(92\)90009-X](https://doi.org/10.1016/0273-2300(92)90009-X), 1992.
- 949 [Oros, D. R., Abas, M. R. bin, Omar, N. Y. M. J., Rahman, N. A. and Simoneit, B. R. T.:](#) Identification and emission factors of molecular tracers in organic aerosols from biomass burning: Part 3. Grasses, *Appl. Geochemistry*, 21(6), 919–940, <https://doi.org/10.1016/j.apgeochem.2006.01.008>, 2006.
- 950 [Orozco, C., Sanandres, E. and Molinares, I.:](#) Colombia, Panamá y la Ruta Panamericana: Encuentros y Desencuentros, *Memorias Rev. Digit. Hist. y Arqueol. desde el Caribe*, 16(ISSN 1794-8886) [http://www.scielo.org.co/scielo.php?script=sci\\_arttext&pid=S1794-88862012000100005](http://www.scielo.org.co/scielo.php?script=sci_arttext&pid=S1794-88862012000100005), last access: 23 February 2022, 2012.
- 951 [Ortiz, E. Y., Jimenez, R., Fochesatto, G. J. and Morales-Rincon, L. A.:](#) Caracterización de la turbulencia atmosférica en una gran zona verde de una megaciudad andina tropical, *Rev. la Acad. Colomb. Ciencias Exactas, Físicas y Nat.*, 43(166), 133, <https://doi.org/10.18257/raccefyn.697>, 2019.
- 952 [Pant, P. and Harrison, R. M.:](#) Estimation of the contribution of road traffic emissions to particulate matter concentrations from field measurements: A review, *Atmos. Environ.*, 77, 78–97, <https://doi.org/10.1016/j.atmosenv.2013.04.028>, 2013.

Con formato: Español (Colombia)

Con formato: Español (Colombia)

Con formato: Español (Colombia)

Con formato: Español (Colombia)

Con formato: Español (Colombia)

- 972 Pereira, G. M., Teinilä, K., Custódio, D., Gomes Santos, A., Xian, H., Hillamo, R., Alves, C. A., Bittencourt de Andrade, J.,  
 973 Olímpio da Rocha, G., Kumar, P., Balasubramanian, R., Andrade, M. de F. and de Castro Vasconcellos, P.: Particulate  
 974 pollutants in the Brazilian city of São Paulo: 1-year investigation for the chemical composition and source apportionment,  
 975 *Atmos. Chem. Phys.*, 17(19), 11943–11969, <https://doi.org/10.5194/acp-17-11943-2017>, 2017.
- 976 Pereira, G. M., Oraggio, B., Teinilä, K., Custódio, D., Huang, X., Hillamo, R., Alves, C. A., Balasubramanian, R., Rojas, N.  
 977 Y. and Sanchez-Cocoylo, O.: A comparative chemical study of PM 10 in three Latin American cities : Lima, Medellín, ans São  
 978 Paulo, *Air Qual. Atmos. Heal.*, 12, 1141–1152, <https://doi.org/10.1007/s11869-019-00735-3>, 2019.
- 979 Pio, C., Cerqueira, M., Harrison, R. M., Nunes, T., Mirante, F., Alves, C., Oliveira, C., Sanchez de la Campa, A., Artfñano, B.  
 980 and Matos, M.: OC/EC ratio observations in Europe: Re-thinking the approach for apportionment between primary and  
 981 secondary organic carbon, *Atmos. Environ.*, 45(34), 6121–6132, <https://doi.org/10.1016/j.atmosenv.2011.08.045>, 2011.
- 982 Plaza, J., Artfñano, B., Salvador, P., Gómez-Moreno, F. J., Pujadas, M. and Pio, C. A.: Short-term secondary organic carbon  
 983 estimations with a modified OC/EC primary ratio method at a suburban site in Madrid (Spain), *Atmos. Environ.*, 45(15), 2496–  
 984 2506, <https://doi.org/10.1016/j.atmosenv.2011.02.037>, 2011.
- 985 Pye, H. O. T., Nenes, A., Alexander, B., Ault, A. P., Barth, M. C., Clegg, S. L., Collett, J. L., Fahey, K. M., Hennigan, C. J.,  
 986 Herrmann, H., Kanakidou, M., Kelly, J. T., Ku, I. T., Faye McNeill, V., Riemer, N., Schaefer, T., Shi, G., Tilgner, A., Walker,  
 987 J. T., Wang, T., Weber, R., Xing, J., Zaveri, R. A. and Zuend, A.: The acidity of atmospheric particles and clouds., 2020.
- 988 Ramírez, O., Sánchez de la Campa, A. M., Amato, F., Catacolí, R. A., Rojas, N. Y. and de la Rosa, J.: Chemical composition  
 989 and source apportionment of PM10 at an urban background site in a high-altitude Latin American megacity (Bogota,  
 990 Colombia), *Environ. Pollut.*, 233, 142–155, <https://doi.org/10.1016/j.envpol.2017.10.045>, 2018.
- 991 Ravindra, K., Sokhi, R. and Van Grieken, R.: Atmospheric polycyclic aromatic hydrocarbons: Source attribution, emission  
 992 factors and regulation, *Atmos. Environ.*, 42(13), 2895–2921, <https://doi.org/10.1016/j.atmosenv.2007.12.010>, 2008.
- 993 Romero, D., Sarmiento, H. and Pachón, J. E.: Estimación de hidrocarburos aromáticos policíclicos y metales pesados asociados  
 994 con la quema de caña de azúcar en el valle geográfico del río Cauca , Colombia, *Rev. Épsilon*, 21(2013), 57–82, 2013.
- 995 Ryu, S. Y., Kim, J. E., Zhuanshi, H., Kim, Y. J. and Kang, G. U.: Chemical composition of post-harvest biomass burning  
 996 aerosols in gwangju, Korea, *J. Air Waste Manag. Assoc.*, 54(9), 1124–1137,  
 997 <https://doi.org/10.1080/10473289.2004.10471018>, 2004.
- 998 Dos Santos, C. Y. M., Azevedo, D. de A. and De Aquino Neto, F. R.: Selected organic compounds from biomass burning  
 999 found in the atmospheric particulate matter over sugarcane plantation areas, *Atmos. Environ.*, 36(18), 3009–3019,  
 1000 [https://doi.org/10.1016/S1352-2310\(02\)00249-2](https://doi.org/10.1016/S1352-2310(02)00249-2), 2002.
- 1001 Schauer, J. J.: Sources contributions to atmospheric organic compound concentrations: Emissions measurements and model  
 1002 predictions, California Institute Technology, 1998.
- 1003 SDA: Plan decenal de descontaminación del aire de Bogotá, Bogotá D.C.  
 1004 [http://ambientebogota.gov.co/en/c/document\\_library/get\\_file?uuid=b5f3e23f-9c5f-40ef-912a-](http://ambientebogota.gov.co/en/c/document_library/get_file?uuid=b5f3e23f-9c5f-40ef-912a-)

Con formato: Español (Colombia)

Con formato: Español (Colombia)

- 1005 51a5822da320&groupId=55886, 2010.
- 1006 Seinfeld, J. H. and Pandis, S. N.: Atmospheric From Air Pollution to Climate Change., 2006.
- 1007 SICOM: Boletín estadístico, Boletín Estad. EDS automotriz y Fluv. <https://www.sicom.gov.co/index.php/boletin-estadistico>,  
1008 last access: 15 February 2022, 2018.
- 1009 Simoneit, B. R. T.: Biomass burning - A review of organic tracers for smoke from incomplete combustion, *Appl.*  
1010 *Geochemistry*, 17(3), 129–162, [https://doi.org/10.1016/S0883-2927\(01\)00061-0](https://doi.org/10.1016/S0883-2927(01)00061-0), 2002.
- 1011 Snider, G., Weagle, C. L., Murdymootoo, K. K., Ring, A., Ritchie, Y., Stone, E., Walsh, A., Akoshile, C., Anh, N. X.,  
1012 Balasubramanian, R., Brook, J., Qonitan, F. D., Dong, J., Griffith, D., He, K., Holben, B. N., Kahn, R., Lagrosas, N., Lestari,  
1013 P., Ma, Z., Misra, A., Norford, L. K., Quel, E. J., Salam, A., Schichtel, B., Segev, L., Tripathi, S., Wang, C., Yu, C., Zhang,  
1014 Q., Zhang, Y., Brauer, M., Cohen, A., Gibson, M. D., Liu, Y., Martins, J. V., Rudich, Y. and Martin, R. V.: Variation in global  
1015 chemical composition of PM<sub>2.5</sub>: emerging results from SPARTAN, *Atmos. Chem. Phys.*, 16(15), 9629–9653,  
1016 <https://doi.org/10.5194/acp-16-9629-2016>, 2016.
- 1017 Sorooshian, A., Crosbie, E., Maudlin, L. C., Youn, J., Wang, Z., Shingler, T., Ortega, A. M., Hersey, S. and Woods, R. K.:  
1018 Surface and airborne measurements of organosulfur and methanesulfonate over the western United States and coastal areas, *J.*  
1019 *Geophys. Res. Atmos.*, 8535–8548, <https://doi.org/10.1002/2015JD023822>.Received, 2015.
- 1020 Souza, D. Z., Vasconcellos, P. C., Lee, H., Aurela, M., Saarnio, K., Teinilä, K. and Hillamo, R.: Composition of PM<sub>2.5</sub> and  
1021 PM<sub>10</sub> collected at Urban Sites in Brazil, *Aerosol Air Qual. Res.*, 14(1), 168–176, <https://doi.org/10.4209/aaqr.2013.03.0071>,  
1022 2014.
- 1023 Stahl, C., Cruz, M. T., Bañaga, P. A., Betito, G., Braun, R. A., Aghdam, M. A., Cambaliza, M. O., Lorenzo, G. R., Macdonald,  
1024 A. B., Hilario, M. R. A., Pabroa, P. C., Yee, J. R. and Simpas, J. B.: Sources and characteristics of size-resolved particulate  
1025 organic acids and methanesulfonate in a coastal megacity : Manila , Philippines, , 15907–15935, 2020.
- 1026 Sutton, M. A., Billen, G., Bleeker, A., Erisman, J. W., Grennfelt, P., Grinsven, H. Van, Grizzetti, B., Howard, C. M. and Leip,  
1027 A.: Technical summary Part I Nitrogen in Europe : the present position, *Eur. Nitrogen Assess. Sources, Eff. Policy Perspect.*,  
1028 (December 2015), Xxxv–Lii, <https://doi.org/10.1017/CBO9780511976988.003>, 2011.
- 1029 Szabó, J., Szabó Nagy, A. and Erdős, J.: Ambient concentrations of PM<sub>10</sub>, PM<sub>10</sub>-bound polycyclic aromatic hydrocarbons  
1030 and heavy metals in an urban site of Győr, Hungary, *Air Qual. Atmos. Heal.*, 8(2), 229–241, [https://doi.org/10.1007/s11869-](https://doi.org/10.1007/s11869-015-0318-7)  
1031 015-0318-7, 2015.
- 1032 Tang, M., Guo, L., Bai, Y., Huang, R., Wu, Z. and Wang, Z.: Impacts of methanesulfonate on the cloud condensation  
1033 nucleation activity of sea salt aerosol, *Atmos. Environ.*, 201(October 2018), 13–17,  
1034 <https://doi.org/10.1016/j.atmosenv.2018.12.034>, 2019.
- 1035 Tobiszewski, M. and Namieśnik, J.: PAH diagnostic ratios for the identification of pollution emission sources, *Environ. Pollut.*,  
1036 162(November 2018), 110–119, <https://doi.org/10.1016/j.envpol.2011.10.025>, 2012.
- 1037 Tsigaridis, K., Daskalakis, N., Kanakidou, M., Adams, P. J., Artaxo, P., Bahadur, R., Balkanski, Y., Bauer, S. E., Bellouin,

Con formato: Español (Colombia)

- 1038 N., Benedetti, A., Bergman, T., Berntsen, T. K., Beukes, J. P., Bian, H., Carslaw, K. S., Chin, M., Curci, G., Diehl, T., Easter,  
 1039 R. C., Ghan, S. J., Gong, S. L., Hodzic, A., Hoyle, C. R., Iversen, T., Jathar, S., Jimenez, J. L., Kaiser, J. W., Kirkevåg, A.,  
 1040 Koch, D., Kokkola, H., Lee, Y., Lin, G., Liu, X., Luo, G., Ma, X., Mann, G. W., Mihalopoulos, N., Morcrette, J. J., Müller,  
 1041 J. F., Myhre, G., Myriokefalitakis, S., Ng, N. L., O'donnell, D., Penner, J. E., Pozzoli, L., Pringle, K. J., Russell, L. M., Schulz,  
 1042 M., Sciare, J., Seland, Shindell, D. T., Sillman, S., Skeie, R. B., Spracklen, D., Stavrou, T., Steenrod, S. D., Takemura, T.,  
 1043 Tiitta, P., Tilmes, S., Tost, H., Van Noije, T., Van Zyl, P. G., Von Salzen, K., Yu, F., Wang, Z., Wang, Z., Zaveri, R. A.,  
 1044 Zhang, H., Zhang, K., Zhang, Q. and Zhang, X.: The AeroCom evaluation and intercomparison of organic aerosol in global  
 1045 models, *Atmos. Chem. Phys.*, 14(19), 10845–10895, <https://doi.org/10.5194/acp-14-10845-2014>, 2014.
- 1046 Turpin, B. J. and Lim, H.: Species Contributions to PM<sub>2.5</sub> Mass Concentrations : Revisiting Common Assumptions for  
 1047 Estimating Organic Mass, *Aerosol Sci. Technol.*, 35:1(September 2014), 37–41,  
 1048 <https://doi.org/http://dx.doi.org/10.1080/02786820119445>, 2010.
- 1049 Urban, R. C., Alves, C. A., Allen, A. G., Cardoso, A. A., Queiroz, M. E. C. and Campos, M. L. A. M.: Sugar markers in aerosol  
 1050 particles from an agro-industrial region in Brazil, *Atmos. Environ.*, 90(2014), 106–112,  
 1051 <https://doi.org/10.1016/j.atmosenv.2014.03.034>, 2014.
- 1052 Urban, R. C., Alves, C. A., Allen, A. G., Cardoso, A. A. and Campos, M. L. A. M.: Organic aerosols in a Brazilian agro-  
 1053 industrial area: Speciation and impact of biomass burning, *Atmos. Res.*, 169, 271–279,  
 1054 <https://doi.org/10.1016/j.atmosres.2015.10.008>, 2016.
- 1055 Vargas, F. A., Rojas, N. Y., Pachon, J. E. and Russell, A. G.: PM<sub>10</sub> characterization and source apportionment at two  
 1056 residential areas in Bogota, *Atmos. Pollut. Res.*, 3(1), 72–80, <https://doi.org/10.5094/APR.2012.006>, 2012.
- 1057 Vasconcellos, P. C., Balasubramanian, R., Bruns, R. E., Sanchez-Ccoyllo, O., Andrade, M. F. and Flues, M.: Water-soluble  
 1058 ions and trace metals in airborne particles over urban areas of the state of São Paulo, Brazil: Influences of local sources and  
 1059 long range transport, *Water, Air, Soil Pollut.*, 186(1–4), 63–73, <https://doi.org/10.1007/s11270-007-9465-2>, 2007.
- 1060 Vasconcellos, P. C., Souza, D. Z., Ávila, S. G., Araújo, M. P., Naoto, E., Nascimento, K. H., Cavalcante, F. S., Dos, M.,  
 1061 Smichowski, P. and Behrentz, E.: Comparative study of the atmospheric chemical composition of three South American cities,  
 1062 *Atmos. Environ.*, 45(32), 5770–5777, <https://doi.org/10.1016/j.atmosenv.2011.07.018>, 2011.
- 1063 Victoria, J., Amaya, A., Rangel, H., Viveros, C., Cassalet, C., Carbonell, J., Quintero, R., Cruz, R., Isaacs, C., Larrahondo, J.,  
 1064 Moreno, C., Palma, A., Posada, C., Villegas, F. and Gómez, L.: Características agronómicas y de productividad de la variedad  
 1065 Cenicaña Colombiana (CC) 85-92, Cali., 2002.
- 1066 Villalobos, A. M., Barraza, F., Jorquera, H. and Schauer, J. J.: Chemical speciation and source apportionment of fine particulate  
 1067 matter in Santiago, Chile, 2013, *Sci. Total Environ.*, 512–513, 133–142, <https://doi.org/10.1016/j.scitotenv.2015.01.006>, 2015.
- 1068 Wadinga Fomba, K., Deabji, N., El Islam Barcha, S., Ouchen, I., Mehdi Elbaramoussi, E., Cherkaoui El Moursli, R., Harnafi,  
 1069 M., El Hajjaji, S., Mellouki, A. and Herrmann, H.: Application of TXRF in monitoring trace metals in particulate matter and  
 1070 cloud water, *Atmos. Meas. Tech.*, 13(9), 4773–4790, <https://doi.org/10.5194/amt-13-4773-2020>, 2020.

Con formato: Español (Colombia)

- 1071 Wagner, R., Jähn, M. and Schepanski, K.: Wildfires as a source of airborne mineral dust - Revisiting a conceptual model using  
1072 large-eddy simulation (LES), *Atmos. Chem. Phys.*, 18(16), 11863–11884, <https://doi.org/10.5194/acp-18-11863-2018>, 2018.
- 1073 Wang, Y., Yang, F., Li, X., Tian, M. and Hopke, P. K.: On the source contribution to Beijing PM<sub>2.5</sub> concentrations, , 134, 84–  
1074 95, <https://doi.org/10.1016/j.atmosenv.2016.03.047>, 2016.
- 1075 WHO Regional Office for Europe: Air quality guidelines for Europe, pp. 457–465, World Health Organization, Copenhagen,  
1076 Denmark, <https://doi.org/10.1525/9780520948068-070>, , 2020.
- 1077 World Health Organization: Review of evidence on health aspects of air pollution - REVIHAAP Project.  
1078 [http://www.euro.who.int/pubrequest%0Ahttp://www.euro.who.int/\\_data/assets/pdf\\_file/0004/193108/REVIHAAP-Final-](http://www.euro.who.int/pubrequest%0Ahttp://www.euro.who.int/_data/assets/pdf_file/0004/193108/REVIHAAP-Final-technical-report-final-version.pdf)  
1079 [technical-report-final-version.pdf](http://www.euro.who.int/pubrequest%0Ahttp://www.euro.who.int/_data/assets/pdf_file/0004/193108/REVIHAAP-Final-technical-report-final-version.pdf), 2013.
- 1080 World Health Organization: WHO global air quality guidelines: particulate matter (PM<sub>2.5</sub> and PM<sub>10</sub>), ozone, nitrogen dioxide,  
1081 sulfur dioxide and carbon monoxide, World Health Organization. <https://www.who.int/publications/i/item/9789240034228>,  
1082 last access: 22 February 2022, 2021.
- 1083 Wu, C. and Zhen Yu, J.: Evaluation of linear regression techniques for atmospheric applications: The importance of appropriate  
1084 weighting, *Atmos. Meas. Tech.*, 11(2), 1233–1250, <https://doi.org/10.5194/amt-11-1233-2018>, 2018.
- 1085 Xue, J., Lau, A. K. H. and Yu, J. Z.: A study of acidity on PM<sub>2.5</sub> in Hong Kong using online ionic chemical composition  
1086 measurements, *Atmos. Environ.*, 45(39), 7081–7088, <https://doi.org/10.1016/j.atmosenv.2011.09.040>, 2011.
- 1087 Yadav, I. C. and Devi, N. L.: Biomass burning, regional air quality, and climate change, *Encycl. Environ. Heal.*, (April), 386–  
1088 391, <https://doi.org/10.1016/B978-0-12-409548-9.11022-X>, 2019.
- 1089 Yadav, S., Tandon, A. and Attri, A. K.: Monthly and seasonal variations in aerosol associated n-alkane profiles in relation to  
1090 meteorological parameters in New Delhi, India, *Aerosol Air Qual. Res.*, 13(1), 287–300,  
1091 <https://doi.org/10.4209/aaqr.2012.01.0004>, 2013.
- 1092 Yan, J., Wang, L., Fu, P. P. and Yu, H.: Photomutagenicity of 16 polycyclic aromatic hydrocarbons from the US EPA priority  
1093 pollutant list, *Mutat. Res. - Genet. Toxicol. Environ. Mutagen.*, 557(1), 99–108,  
1094 <https://doi.org/10.1016/j.mrgentox.2003.10.004>, 2004.
- 1095 Yunker, M. B., Macdonald, R. W., Vingarzan, R., Mitchell, H., Goyette, D. and Sylvestre, S.: PAHs in the Fraser River basin:  
1096 a critical appraisal of PAH ratios as indicators of PAH source and composition, *Org. Geochem.*, 33, 489–515,  
1097 [https://doi.org/doi.org/10.1016/S0146-6380\(02\)00002-5](https://doi.org/doi.org/10.1016/S0146-6380(02)00002-5), 2002.
- 1098

Con formato: Español (Colombia)